Asymmetric self-interacting dark matter via Dirac leptogenesis

Manoranjan Dutta[1,*] Nimmala Narendra[2,†] Narendra Sahu[3,‡] and Sujay Shil[4,5,6,7,§]

[1] *Department of Physics, North Lakhimpur College (Autonomous), Khelmati, North Lakhimpur, Lakhimpur, Assam 787031, India*
[2] *Theoretical Physics Division, Physical Research Laboratory, Ahmedabad 380009, India*
[3] *Department of Physics, Indian Institute of Technology, Hyderabad, Kandi, Sangareddy 502284, Telangana, India*
[4] *IIT Gandhinagar, Palaj Campus, Gujarat 382355, India*
[5] *Institute of Physics, Sachivalaya Marg, Bhubaneswar 751005, Odisha, India*
[6] *Homi Bhabha National Institute, BARC Training School Complex, Anushakti Nagar, Mumbai 400094, India*
[7] *Instituto de Física, Universidade de São Paulo, Rua do Matão 1371, 05508-090 São Paulo, Brazil*

(Received 5 April 2022; accepted 19 October 2022; published 15 November 2022)

The nature of neutrinos, whether Dirac or Majorana, is hitherto not known. Assuming that the neutrinos are Dirac, which needs $B-L$ to be an exact symmetry, we make an attempt to explain the observed proportionality between the relic densities of dark matter (DM) and baryonic matter in the present Universe i.e., $\Omega_{\rm DM} \approx 5\Omega_{\rm B}$. We extend the Standard Model (SM) by introducing heavy scalar doublets X_i, $i = 1$, 2 and η, two singlet scalars Φ and Φ', a vectorlike Dirac fermion χ representing the DM and three right-handed neutrinos ν_{R_i}, $i = 1$, 2, 3. Assuming $B-L$ is an exact symmetry of the early Universe, the CP-violating out-of-equilibrium decay of heavy scalar doublets; X_i, $i = 1$, 2 to the SM lepton doublet L and the right-handed neutrino ν_R, generate equal and opposite $B-L$ asymmetry among left (ν_L) and right (ν_R)-handed neutrinos. We ensure that $\nu_L - \nu_R$ equilibration does not occur until below the electroweak (EW) phase transition during which a part of the lepton asymmetry gets converted to dark matter asymmetry through a dimension eight operator, which conserves $B-L$ symmetry and remains in thermal equilibrium above sphaleron decoupling temperature. A part of the remaining $B-L$ asymmetry then gets converted to a net B asymmetry through EW-sphalerons which are active at a temperature above 100 GeV. To alleviate the small-scale anomalies of ΛCDM, we assume the DM (χ) to be self-interacting via a light mediator Φ, which not only depletes the symmetric component of the DM, but also paves a way to detect the DM at terrestrial laboratories through $\Phi - H$ mixing, where H is the SM Higgs doublet.

DOI: 10.1103/PhysRevD.106.095017

I. INTRODUCTION

It is presumed that the early Universe has gone through a period of exponential expansion called inflation to solve the cosmological problems. At the end of inflation, the Universe is reheated to give rise to a thermal bath with reheating temperature $T_R \gtrsim 4$ MeV in order to facilitate the big bang nucleosynthesis (BBN). It is expected that the different components of the present Universe, such as dark matter, dark energy and baryonic matter must have been cooked in a postinflationary thermal bath. At present, the visible component (baryonic matter) of the Universe is best understood in terms of the standard model (SM) of particle physics, which is based on the gauge group $SU(3)_c \times SU(2)_L \times U(1)_Y$. However, the SM fails to explain many other aspects of the observed Universe, such as baryon asymmetry, dark matter, dark energy, nonzero but small neutrino mass etc.

Within the framework of the SM, neutrinos are exactly massless. However, the solar and atmospheric neutrino oscillation experiments hint towards the nonzero masses and mixings of light neutrinos. In fact, this has been further confirmed by relatively recent oscillation experiments like T2K [1,2], Double Chooz [3,4], Daya Bay [5–7], Reno [8], and MINOS [9,10]. For a recent global fit of neutrino oscillation experiment, we refer to [11]. The neutrino

[*] dutta.manoranjan@nlc.ac.in
[†] nnarendra@prl.res.in
[‡] nsahu@phy.iith.ac.in
[§] sujay.s@iitgn.ac.in

masses are also further constrained by cosmology. The cosmic microwave background radiation data give an upper bound on the sum of light neutrino masses to be $\sum_i |m_i| < 0.12$ eV [12]. Thus the data from various sources imply that neutrinos have mass. However, the nature of neutrino mass, whether Dirac or Majorana, is not confirmed yet. If the neutrinos are Majorana, which implies lepton number is violated by two units, then the seesaw mechanisms: type-I [13–16], type-II [17–23], type-III [24] or their variants [25] are the best theoretical candidates to get their sub-eV masses. It is important to note that all these seesaw mechanisms and their variants introduce additional heavy particles to the SM. After integrating out the heavy degrees of freedom we get the effective dimension five operator $LLHH/\Lambda$, where L, H are lepton and Higgs doublets of the SM and Λ is the mass scale of heavy degrees of freedom introduced in the various seesaw mechanisms. After electroweak phase transition, the dimension-five operator generates sub-eV Majorana masses of neutrinos. On the other hand, if the neutrinos are Dirac, then lepton number is an exact symmetry of nature as it stands now in the SM. In this case, the sub-eV masses of light neutrinos imply that the Yukawa coupling involving $\bar{L}\tilde{H}N_R$, with N_R being the singlet right-handed neutrino, is of $\mathcal{O}(10^{-12})$, which is almost six orders of magnitude less than the electron Yukawa coupling. Thus the sub-eV Dirac mass of light neutrinos requires substantial fine tuning.

Another important aspect of the SM is the identity of dark matter, which plays a major role throughout the evolution of the Universe. Astrophysical evidences from galaxy rotation curve, gravitational lensing and large-scale structure of the Universe confirmed the existence of dark matter [26,27]. In fact, the satellite-borne experiments WMAP [28] and Planck [29], which measure the temperature fluctuation in the cosmic microwave background (CMBR), precisely determine the relic abundance of baryon and dark matter (DM) to be $\Omega_B h^2 = 0.02237 \pm 0.00015$ and $\Omega_{DM} h^2 = 0.1200 \pm 0.0012$ respectively at 68% CL, where Ω_{DM} is the density parameter and $h =$ Hubble Parameter$/(100\ \mathrm{km\,s^{-1}\,Mpc^{-1}})$ is the reduced Hubble constant. This implies that the DM abundance is about five times the baryon abundance: i.e., $\Omega_{DM} \approx 5\Omega_B$. While it is very natural for the Universe to start in a baryon symmetric manner, the present Universe is highly baryon asymmetric, giving rise to the long-standing puzzle of the baryon asymmetry of the Universe (BAU). The observed BAU is quantitatively expressed by the ratio of baryon density over antibaryons density to photon density as [30]

$$\eta_B = \frac{n_B - n_{\bar{B}}}{n_\gamma} \simeq 6.2 \times 10^{-10}. \tag{1}$$

The origin of this asymmetry is also not known along with the particle nature of DM.

In the well-established ΛCDM model, DM is assumed to be cold and collisionless which is supposed to have facilitated the structure formation in the early Universe by providing the necessary gravitational potential for primordial density fluctuations to grow. However, cosmological simulations in recent times reveal a few severe discrepancies of the ΛCDM model at small scales, leading to anomalies such as the cusp-core problem, missing satellite problem and too-big-to-fail problem [31,32]. To alleviate these small-scale ΛCDM anomalies, Spergel and Steinhardt proposed in 2000 an interesting alternative to cold dark matter (CDM) in terms of self-interacting dark matter (SIDM) [33]. Earlier studies in this direction can be found in [34,35]. SIDM can have large self-scattering cross sections of $\mathcal{O}(10^{-24}\ \mathrm{cm^2/GeV})$ [36–41], which is way too larger than typical cross section of $\mathcal{O}(10^{-38}\ \mathrm{cm^2/GeV})$ for weakly interacting massive particles (WIMPs), a well-suited class of candidates for CDM scenario. Such large self-interacting cross sections of DM can be naturally realized in scenarios where DM has a light mediator. In such a scenario, self-interaction is stronger for smaller DM velocities such that it can have a large impact on small scale structures, while it gets reduced at larger scales due to large velocities of DM and hence remains consistent with large scale CDM predictions [36–39,42–45]. The light mediator also mixes with the SM Higgs paving a way for detecting DM at direct detection experiments [46,47]. Several model building efforts have been made to realize such scenarios, see [48–58] and references therein.

Thus, both the SM and the ΛCDM models are inadequate to explain a plethora of mysteries in physics. At present, the nature of neutrinos, either Dirac or Majorana, is not confirmed yet. In future, the neutrinoless double beta decay experiments [59] may shed light on it. In this paper, assuming neutrinos to be Dirac (i.e., $B - L$ is an exact symmetry) and the DM to be self-interacting, we make an attempt to explain simultaneously the three most puzzling physical phenomena viz. neutrino mass, DM and the baryon asymmetry of the Universe along with a natural explanation of the ratio $\Omega_{DM} \approx 5\Omega_B$. We extend the SM with heavy $SU(2)_L$ scalar doublets X_i, $(i = 1, 2)$, and η, singlet right-handed neutrinos ν_{iR}, $(i = 1, 2, 3)$ and singlet scalars Φ, Φ' along with a vectorlike singlet Dirac fermion χ which represents the SIDM candidate. Since we assume that $B - L$ is an exact symmetry, the CP-violating out-of-equilibrium decay of the lightest X: i.e., $X \to H\Phi'$ and $X \to L\nu_{iR}$ generates equal and opposite $B - L$ asymmetry between ν_L and ν_R [60–66]. After Φ' and H acquire vacuum expectation values (VEV), we get Dirac mass of neutrinos of appropriate order. By introducing an additional $U(1)_D$ symmetry (which forbids $\bar{L}\tilde{H}\nu_R$ coupling) we ensure that $\nu_L - \nu_R$ equilibration does not occur until below the electroweak (EW) phase transition during which a part of the lepton asymmetry gets converted to dark matter asymmetry through a dimension eight operator:

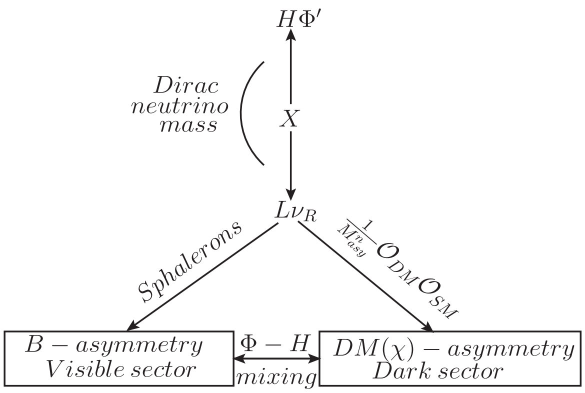

FIG. 1. Pictorial representation shows: (i) the generation of neutrino mass, (ii) the generation of the $B-L$ asymmetry in the lepton sector. The sphalerons above electroweak (EW) phase transition ($T_{\rm EW}$) transfers a part of $B-L$ asymmetry to the observed B-asymmetry, while the higher dimension operator $\mathcal{O}_8$ is in thermal equilibrium above EW-phase transition, at $T > T_{\rm EW}$, cooks a net DM asymmetry out of the existing $B-L$ asymmetry. The $\Phi-H$ mixing provides a bridge between the visible and dark sectors.

$\mathcal{O}_8 = \frac{1}{M_{\rm asy}^4}\bar{\chi}^2(LH)^2$ [67–71], $M_{\rm asy}$ being fixed by the mass and relevant couplings of η. A part of the remaining $B-L$ asymmetry then gets converted to a net B asymmetry through EW-sphalerons which are active at a temperature above 100 GeV. The singlet scalar Φ not only mediates the self-interaction among the DM particles, but also helps in depleting the symmetric component of the DM. Moreover it mixes with the SM Higgs providing a portal for detecting the DM at terrestrial laboratories. We constrain the scalar portal mixing with recent data from experiments like CRESST-III and XENON1T. The pictorial presentation can be seen in Fig. 1.

The paper is arranged as follows. In Sec. II, we explain the model for simultaneous explanation of SIDM, baryon asymmetry and Dirac mass of the light neutrinos. In Sec. III, we explain the Dirac leptogenesis mechanism and production as well as relic density of DM. In Sec. IV, we find the parameter space for sufficient self-interaction with desired velocity dependence followed by a discussion on the direct detection prospects of the SIDM in Sec. V. In Sec. VI, we discuss the parameter space for light neutrino mass and conclude in Sec. VII.

II. THE MODEL

We extend the SM, which is based on the gauge group: $SU(3)_c \times SU(2)_L \times U(1)_Y$, with $U(1)_D \times U(1)_{B-L}$ global symmetries. The particle contents of the model are shown in Table I along with their quantum numbers under the imposed symmetry. The scalar sector consists of heavy scalar doublets X_i, $(i = 1, 2)$ and η, and two singlet scalars Φ, Φ'; while the fermion sector consists of a vectorlike Dirac fermion χ along with three heavy right-handed neutrinos ν_{R_i}, $(i = 1, 2, 3)$, all singlet under the SM gauge group. All these particles carry nontrivial charges under $U(1)_D$ symmetry, while the SM particles remain neutral. Under the extended symmetries, the Majorana mass terms of χ and ν_R are forbidden.

Owing to the symmetry and the charge assignment as shown in Table I, the Lagrangian of the model can be written as[1]

$$-\mathcal{L} \supset m_\chi\bar{\chi}\chi + \lambda_D\bar{\chi}\chi\Phi + y\bar{L}\,\tilde{\chi}\,\nu_R + \rho\Phi'^* X^\dagger H + \lambda\bar{\chi}L\eta + \text{H.c.} + V(X, \eta, H, \Phi, \Phi'), \tag{2}$$

where

$$\begin{aligned} V(\eta, H, \Phi, \Phi') = {} & M_\eta^2(\eta^\dagger\eta) + \lambda_\eta(\eta^\dagger\eta)^2 + \lambda'_{\eta H}(\eta^\dagger\eta)(H^\dagger H) + [\lambda_{\eta H}(\eta^\dagger H)^2 + \text{H.c.}] \\ & - \mu_H^2 H^\dagger H + \lambda_H(H^\dagger H)^2 + \frac{1}{2}m_\phi^2\Phi^2 + \frac{1}{3}\mu_\Phi\Phi^3 + \frac{1}{4}\lambda_\Phi\Phi^4 - \mu_\Phi^2(\Phi'^\dagger\Phi') + \lambda_{\Phi'}(\Phi'^\dagger\Phi')^2 \\ & + \frac{\mu_1}{\sqrt{2}}\Phi H^\dagger H + \frac{\mu_2}{\sqrt{2}}\Phi(\Phi'^\dagger\Phi') + \frac{\lambda_H\Phi}{2}H^\dagger H\Phi^2 + \lambda_{H\Phi'}H^\dagger H(\Phi'^\dagger\Phi') + \frac{\lambda\Phi\Phi'}{2}\Phi^2(\Phi'^\dagger\Phi'). \end{aligned} \tag{3}$$

The term $\lambda_{\eta H}(\eta^\dagger H)^2 + \text{H.c.}$ in the potential (3), breaks the $U(1)_D$ symmetry softly to a remnant Z_2 symmetry under which η and χ are odd, while all other particles are even. We assume that η doesn't acquire a VEV in order to preserve the remnant Z_2 symmetry. Considering $M_\eta \gg M_\chi$, χ becomes the viable DM candidate. In this way, we ensure

TABLE I. The additional particle content and their quantum numbers under the imposed symmetry.

Fields	$SU(2)_L$	$U(1)_Y$	$U(1)_D$	$U(1)_{B-L}$
X_i	2	+1	−1	0
η	2	+1	1/2	0
ν_R	1	0	−1	−1
Φ'	1	0	+1	0
Φ	1	0	0	0
χ	1	0	1/2	−1

[1]For simplicity we suppress the indices and state when they require explicitly.

the stability to DM χ as well as the theory escapes from having a Goldstone boson.

The Lagrangian terms $\lambda\bar{\chi}L\eta + \lambda_{\eta H}(\eta^\dagger H)^2 + \mathrm{H.c.}$ give rise to a dimension-eight transfer operator via the Feynman diagram shown in top panel of Fig. 2. In the later part of the draft, we will show that this operator transfers the lepton asymmetry from visible sector to dark sector. At low energy, upon integrating out the heavy scalar η, we get the dimension-eight operator [67–71]

$$\mathcal{O}_8 = \frac{\lambda^2\lambda_{\eta H}\bar{\chi}LHH\bar{\chi}L}{M_\eta^4} \equiv \frac{\bar{\chi}^2(LH)^2}{M_{\mathrm{asy}}^4}, \qquad (4)$$

where $M_{\mathrm{asy}}^4 = M_\eta^4/(\lambda^2\lambda_{\eta H})$. Similarly, the Lagrangian terms $y\bar{L}\,\tilde{X}\,\nu_R + \rho\Phi'^{*}X^\dagger H$ lead to an effective dimension-five operator by integrating out the heavy scalar field X at low energy. The Feynman diagram for this dimension-five operator $\mathcal{O}_5 = y\frac{\rho}{M_X^2}\bar{L}H\Phi'\nu_R$ is shown in the bottom panel of Fig. 2.

In writing down the scalar potential as given in Eq. (3), we assume that the scalar doublet X being very heavy, do not participate in low-energy phenomenology and have implications only in leptogenesis. Here $\mu_H^2, m_\phi^2, \mu_{\Phi'}^2 > 0$. We further assume that μ_Φ and λ_Φ are small. As a result, Φ acquires a nonzero VEV through the trilinear terms $\mu_1\Phi(H^\dagger H)$ and $\mu_2\Phi(\Phi'^\dagger\Phi')$, which are proportional to the coupling constants μ_1 and μ_2, respectively. The fluctuations of the fields Φ', H, and Φ around their corresponding VEV's can be written as

$$\Phi' = \frac{w+\phi'}{\sqrt{2}}, \qquad H = \begin{bmatrix} 0 \\ \frac{v+h}{\sqrt{2}} \end{bmatrix} \quad \text{and} \quad \Phi = u + \phi. \qquad (5)$$

From Eq. (3), the stationary conditions are obtained as

$$\begin{aligned} & w\left(-\mu_{\Phi'}^2 + \lambda_{\Phi'}w^2 + \frac{\mu_2}{\sqrt{2}}u + \frac{\lambda_{H\Phi'}}{2}v^2 + \frac{\lambda_{\Phi\Phi'}}{2}u^2\right) = 0, \\ & v\left(-\mu_H^2 + \lambda_H v^2 + \frac{\mu_1}{\sqrt{2}}u + \frac{\lambda_{H\Phi'}}{2}w^2 + \frac{\lambda_{H\Phi}}{2}u^2\right) = 0, \\ & u\left(m_\phi^2 + \mu_\Phi u + \lambda_\Phi u^2 + \frac{\lambda_{H\Phi}}{2}v^2 + \frac{\lambda_{\Phi\Phi'}}{2}w^2\right) \\ & \qquad + \frac{\mu_1}{2\sqrt{2}}v^2 + \frac{\mu_2}{2\sqrt{2}}w^2 = 0. \end{aligned} \qquad (6)$$

Assuming $\mu_\Phi \ll m_\Phi \sim 10^{-3}$ GeV and $\lambda_\Phi \ll 1$, we can drop the terms proportional to $\mathcal{O}(u^2)$ and $\mathcal{O}(u^3)$. In this limit, Eq. (6) can be rewritten as

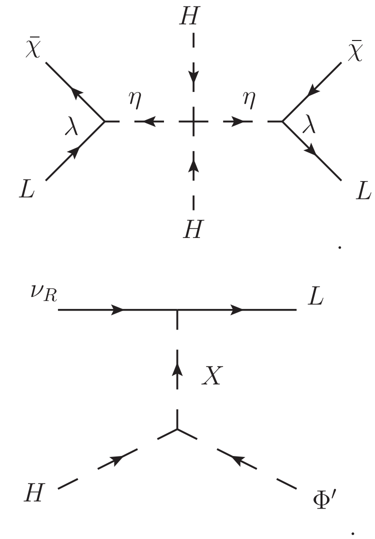

FIG. 2. Top: Feynman diagram of the dimension-eight operator. Bottom: Feynman diagram of the dimension-five operator.

$$\begin{aligned} & w\left(-\mu_{\Phi'}^2 + \lambda_{\Phi'}w^2 + \frac{\mu_2}{\sqrt{2}}u + \frac{\lambda_{H\Phi'}}{2}v^2\right) = 0, \\ & v\left(-\mu_H^2 + \lambda_H v^2 + \frac{\mu_1}{\sqrt{2}}u + \frac{\lambda_{H\Phi'}}{2}w^2\right) = 0, \\ & u\left(m_\phi^2 + \frac{\lambda_{H\Phi}}{2}v^2 + \frac{\lambda_{\Phi\Phi'}}{2}w^2\right) + \frac{\mu_1}{2\sqrt{2}}v^2 + \frac{\mu_2}{2\sqrt{2}}w^2 = 0. \end{aligned} \qquad (7)$$

Thus, the VEVs of the fields Φ', H and Φ are obtained as

$$\begin{aligned} w &= \sqrt{\frac{\mu_{\Phi'}^2 - \frac{\mu_2}{\sqrt{2}}u - \frac{\lambda_{H\Phi'}}{2}v^2}{\lambda_{\Phi'}}}, \\ v &= \sqrt{\frac{\mu_H^2 - \frac{\mu_1}{\sqrt{2}}u - \frac{\lambda_{H\Phi'}}{2}w^2}{\lambda_H}}, \\ u &= \frac{-(\mu_1 v^2 + \mu_2 w^2)}{2\sqrt{2}\left(m_\phi^2 + \frac{\lambda_{H\Phi}}{2}v^2 + \frac{\lambda_{\Phi\Phi'}}{2}w^2\right)}. \end{aligned} \qquad (8)$$

The smallness of u in Eq. (8) can be justified by assuming μ_1, $\mu_2 \to 0$. The squared mass matrix for the neutral components of three scalar fields Φ', H and Φ *viz.* ϕ', h, ϕ can be written in the basis (ϕ', h, ϕ) as

$$\begin{pmatrix} 2\lambda_{\Phi'}w^2 & \frac{1}{2}\lambda_{H\Phi'}vw & \frac{1}{2}(\frac{\mu_2 w}{\sqrt{2}} + \lambda_{\Phi\Phi'}uw) \\ \frac{1}{2}(\lambda_{H\Phi'}vw) & 2\lambda_H v^2 & \frac{1}{2}(\frac{\mu_1 v}{\sqrt{2}} + \lambda_{H\Phi}vu) \\ \frac{1}{2}(\frac{\mu_2 w}{\sqrt{2}} + \lambda_{\Phi\Phi'}uw) & \frac{1}{2}(\frac{\mu_1 v}{\sqrt{2}} + \lambda_{H\Phi}vu) & m_\phi^2 + \frac{\lambda_{H\Phi}}{2}v^2 + \frac{\lambda_{\Phi\Phi'}}{2}w^2 \end{pmatrix}. \qquad (9)$$

As we need light messengers (in MeV scale) to realize sufficiently large DM self-interaction, which also helps in

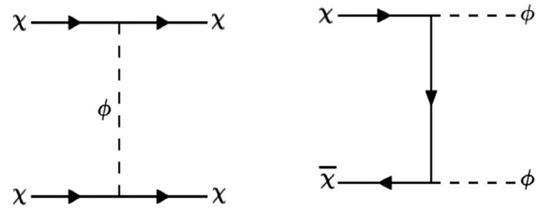

FIG. 3. Left: Feynman diagram for elastic DM self-interaction. Right: Dominant annihilation mode for the symmetric component of DM χ.

annihilating away the symmetric component of DM, we consider the induced VEV u of the field Φ to be very small compared to that of SM Higgs. The details of the diagonalization is given in Appendix B. After complete diagonalization, we are left with three mass eigenstates h_1, h_2, and h_3. The eigenstate h_1 with mass $m_{h_1} \approx m_h = 125.18$ GeV can be identified as the SM Higgs. The eigenstate h_2 with mass $m_{h_2} \sim m_{\Phi'} \sim 10^5$ has implications in addressing the neutrino mass and the extra light scalar h_3 with mass $m_{h_3} \sim m_\phi$ ($\approx$MeV scale) mediates the DM self-interaction and annihilates away the symmetric DM component.

The second term of Eq. (2) gives rise to scalar mediated DM self-interaction via the Feynman diagram shown in the left panel of Fig. 3. The third and fourth terms are responsible for two CP-violating out-of-equilibrium decays, $X \to L\nu_{iR}$ and $X \to H\Phi'$ that generate equal and opposite $B-L$ asymmetry between ν_L and ν_R, required for leptogenesis [72–87]. The dimension-eight operator $\mathcal{O}_8$ remains in thermal equilibrium until below the electroweak phase transition, during which it transfers the lepton number to the DM number in a $B-L$ conserving way in order to establish a proportionality between DM and baryon densities. The strong Yukawa couplings of SM charged leptons rapidly cancel the left and right-handed numbers through the Left-Right equilibration processes. But the situation is different for neutrinos due to their tiny Yukawa couplings. They equilibrate after the sphalerons go out of thermal equilibrium. By that time the sphalerons convert a part of left-handed neutrino asymmetry to the desired B asymmetry [88–95], while the dimension-eight operator $\mathcal{O}_8$ keeps on cooking a net DM asymmetry from the existing neutrino asymmetry [96–127]. This mechanism directly connects the small Dirac neutrino masses to the DM abundance and the baryon asymmetry of the Universe.

The scalar ϕ is sufficiently light and mediates the self-interaction between the DM particles. Interestingly, the symmetric component of DM depletes via its annihilation into ϕ via the Feynman diagram depicted in the right panel of Fig. 3. Moreover, it mixes with the SM Higgs and paves a path to detect the DM at direct-search experiments. The VEVs of singlet scalar $\langle\Phi'\rangle = w$ and SM-Higgs $\langle H\rangle = v$ gives small neutrino masses via higher-dimension operator $\mathcal{O}_5 = y\frac{\rho}{M_X^2}\bar{L}H\Phi'\nu_R$, where the heavy scalar mass suppresses the weak scale.

III. DIRAC LEPTOGENESIS AND THE DM RELIC DENSITY

As the Universe cools down, the heavy scalar doublet X which is assumed to have existed in the early Universe, goes out of thermal equilibrium below its mass scale and decay in a CP-violating way through the channels; $X_1 \to L\nu_R$ and $X_1 \to H\Phi'$ creating an equal and opposite $B-L$ asymmetry in both left- and right-handed sector, see Eq. (2). The total decay rate of X_1 is given by

$$\Gamma_{X_1} = \frac{1}{8\pi}\left(y_1^2 + \frac{\rho_1^2}{M_{X_1}^2}\right)M_{X_1} = \frac{1}{8\pi}(y_1^2 + f_1^2)M_{X_1}, \tag{10}$$

where ρ_1 and y_1 are the trilinear and the Yukawa couplings respectively and in the second line of Eq. (10), we have defined the dimensionless parameter $f_1 = \frac{\rho_1}{M_{X_1}}$, M_{X_1} being the mass of the heavy scalar X_1. To get the adequate lepton asymmetry, the dominant decay channel must be $X_1 \to L\nu_R$, for which the branching ratio $B_L(X_1 \to L\nu_{iR})$ is given by

$$B_L(X_1 \to L\nu_R) = \frac{(y_1^2 M_{X_1})/8\pi}{\Gamma_{X_1}} = \frac{1}{1 + \frac{f_1^2}{y_1^2}}. \tag{11}$$

We assume $B_L(X_1 \to L\nu_R) \sim 0.9$ in order to generate the desired lepton asymmetry. Therefore, f_1 and y_1 differ roughly by an order magnitude. Since parameters f_1 and y_1 are also used in Sec. VI to explain tiny neutrino mass as $y_1 \sim \mathcal{O}(10^{-4})$ and $f_1 \sim \mathcal{O}(10^{-5})$, we stick to region $f_1, y_1 \lesssim 10^{-4}$ in this section. Demanding $\Gamma_{X_1} \lesssim H$ at $T = M_{X_1}$, where $H = 1.67 g_*^{1/2} T^2/M_{\rm Pl}$ is the Hubble expansion parameter, we get $M_{X_1} \lesssim 10^{10}$ GeV for $f_1, y_1 \lesssim 10^{-4}$. For the CP asymmetry to be nonzero, we require at least two doublet scalars X_i, $i = 1, 2$. With just one X, the CP asymmetry will be zero as the imaginary part of the couplings become zero, which can be seen in

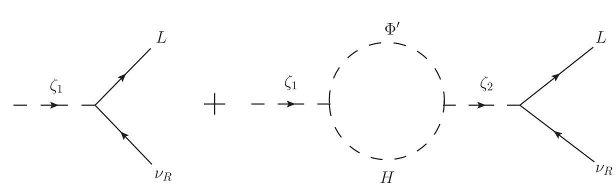

FIG. 4. Tree-level and self-energy correction diagrams, whose interference give arise to a net CP violation in the decay of ζ_1.

Eq. (11). In presence of these doublet scalars and their interactions, they form a mass matrix $M^2_{\pm}$. By diagonalizing this mass matrix, we get new mass eigenstates $\zeta_1^{\pm}$ and $\zeta_2^{\pm}$. See for more details [128,129].

We assume a hierarchy among the masses of $\zeta_1^{\pm}$ and $\zeta_2^{\pm}$ such that the final asymmetry is generated via the decay of the lightest one $\zeta_1^{\pm}$. The CP violation arises via the interference of tree-level and one-loop self-energy correction diagrams of lightest scalar doublet $\zeta_1^{\pm}$ as shown in Fig. 4.

The generated asymmetry in the visible sector is then given by

$$\epsilon_L = [B_L(\zeta_1^- \to l^- \nu_R) - B_L(\zeta_1^+ \to (l^-)^c \nu_R^c)] \\ = -\frac{\mathrm{Im}(\rho_1^* \rho_2 \sum_{k,l} y_{1kl}^* y_{2kl})}{8\pi^2 (M^2_{\zeta_2} - M^2_{\zeta_1})} \left[\frac{M_{\zeta_1}}{\Gamma_{\zeta_1}}\right], \tag{12}$$

where B_L is the branching ratio for $\zeta_1^{\pm} \to l^{\pm} \nu_R$ and $M_{\zeta_i}, i = 1,\, 2$ are the masses of heavy doublet scalars. Here $\rho_{1,2}$ are respectively the mass dimension coupling of $X_{1,2}$ with $\Phi' H$, while $y_{1,2}$ are the respective Yukawa couplings of $X_{1,2}$ with $L\nu_R$. We get a net $B - L$ asymmetry [71,130–132].

$$(n_{B-L})_{\mathrm{total}} = \epsilon_L \kappa s \times \frac{n^{eq}_{\zeta_1}(T \to \infty)}{s}, \tag{13}$$

where $(n^{eq}_{\zeta_1}/s)(T \to \infty) = 135\zeta(3)/(4\pi^4 g_*)$ is the relativistic equilibrium abundance of $\zeta_1^{\pm}$, where $\zeta(3) = 1.202$. $s = (2\pi^2/45) g_* T^3$ is the entropy density of the comoving volume. κ is the washout factor, which arises due to inverse decay and scattering processes. It can vary between 0 to 1 depending on the strength of the Yukawa coupling. For definiteness we choose $\kappa = 0.01$. The $B - L$ asymmetry in the visible sector can be generated by solving the relevant coupled Boltzmann equations given by Eq. (14) [129]. In Fig. 5 we show the evolution of the number density of ζ_1, i.e., Y_{ζ_1} and the $B - L$ asymmetry $Y_{\mathrm{B-L}}$ by solving the Boltzmann equations as given below,

$$\frac{dY_{\zeta_1}}{dx} = -\frac{x}{H(M_{\zeta_1})} s\langle\sigma|v|_{(\zeta_1\zeta_1 \to All)}\rangle [Y^2_{\zeta_1} - (Y^{eq}_{\zeta_1})^2] \\ -\frac{x}{H(M_{\zeta_1})} \Gamma_{(\zeta_1 \to All)} [Y_{\zeta_1} - Y^{eq}_{\zeta_1}] \\ \frac{dY_{\mathrm{B-L}}}{dx} = \frac{x}{H(M_{\zeta_1})} [\epsilon_L \Gamma_{(\zeta_1 \to All)} B_L (Y_{\zeta_1} - Y^{eq}_{\zeta_1}) - \Gamma_W Y_{\mathrm{B-L}}], \tag{14}$$

where Γ_W in the second equation takes care of the washout effects corresponding to inverse decay and scattering. The decay and the inverse decay of $\zeta_1^{\pm}$ are related by $\Gamma_{\mathrm{inv}} = (Y^{eq}_{\zeta_1}/Y^{eq}_{\ell})\Gamma_{(\zeta_1 \to All)}$. The inverse decay of $\zeta_1^{\pm}$ falls exponentially after the latter goes out-of-equilibrium.

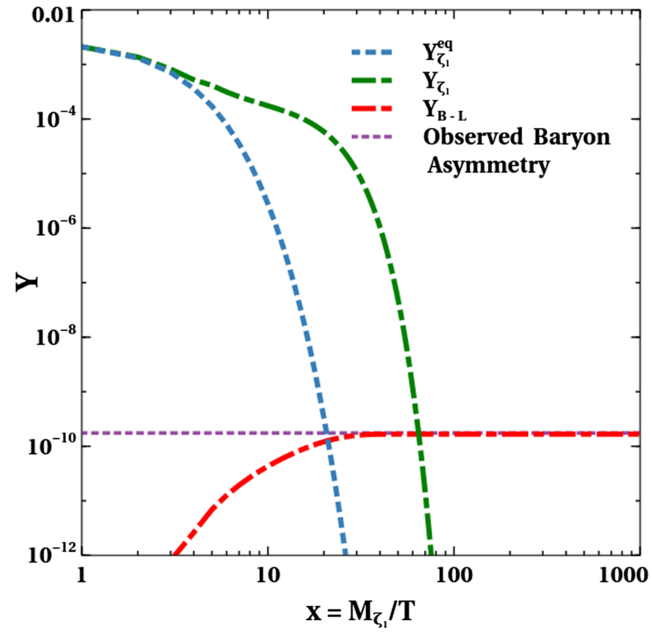

FIG. 5. Abundance of $B - L$ and ζ_1 as a function of dimensionless variable $x = M_{\zeta_1}/T$. The red dot-dashed line shows the abundance of $B - L$ asymmetry, where $\epsilon_L = 10^{-6}$. The green dot-dashed line shows the abundance of ζ_1. The blue dotted line shows the equilibrium abundance of ζ_1. Here, we have taken $y_1 = 10^{-4}$, $\rho_1 = 10^5$ GeV and $M_{\zeta_1} = 10^{10}$ GeV.

Similarly the lepton number conserving $2 \to 2$ scattering processes: $\nu_R \Phi' \to LH$, $\nu_R H \to L\Phi'$, $\nu_R \bar{L} \to H\Phi'$ mediated by X particles are suppressed due to the small Yukawa couplings required for generating light neutrino masses of Dirac type in Sec. VI. The resulting $B - L$ asymmetry is shown by the red dot-dashed line in Fig. 5.

In the following we discuss the distribution of the generated $B - L$ asymmetry between the visible sector and the dark sector. Once the $B - L$ asymmetry is generated in the visible sector, the dimension-8 operator $\mathcal{O}_8 = \frac{1}{M^4_{\mathrm{asy}}} \bar{\chi}^2 (LH)^2$ transfers it partially to the dark sector [68]. This requires the $\mathcal{O}_8$ operator to be in thermal equilibrium above the sphaleron decoupling temperature T_{sph}. For Higgs mass $M_{h_1} = 125$ GeV, $T_{\mathrm{sph}} \gtrsim M_W$, where M_W is the W-boson mass. As discussed in Refs. [71,133], the $\mathcal{O}_8$ operator remains in thermal equilibrium down to a temperature $T_D \gtrsim T_{\mathrm{sph}} = M_W$ for $M_{\mathrm{asy}} \gtrsim 0.9 \times 10^4$ GeV. As a result the DM remains in thermal contact with the visible sector via this $\mathcal{O}_8$ operator down to a decoupling temperature $T_D \gtrsim T_{\mathrm{sph}} = M_W$, during which a net $B - L$ asymmetry of the χ particles is generated.The details of the chemical equilibrium calculation are given in Appendix A. The number density of χ is then given by

$$n_\chi = (n_{\mathrm{B-L}})_{\mathrm{dark}} = \frac{58}{291} (n_{B-L})_{\mathrm{vis}}. \tag{15}$$

The total $B-L$ asymmetry created in the early universe is through out-of-equilibrium decays of ζ_1 and it is the only source of $B-L$ asymmetry in both dark and visible sectors. So we have the following condition,

$$(n_{B-L})_{\text{total}} = (n_{B-L})_{\text{vis}} + (n_{B-L})_{\text{dark}} \\ = \frac{349}{291}(n_{B-L})_{\text{vis}}. \quad (16)$$

Comparing Eq. (16) with Eq. (13) and using $n_{\text{B}} = 0.31(n_{\text{B-L}})_{\text{vis}}$ [71], we get the required CP asymmetry for observed lepton abundance to be $\epsilon_L = 141.23(\eta/\kappa)$. For $\kappa \sim 0.01$, the required CP asymmetry is $\epsilon_L \sim 10^{-6}$. Using Eq. (16) in $n_{\text{B}} = 0.31(n_{\text{B-L}})_{\text{vis}}$ and Eq. (15) we get

$$n_{\text{B}} = \frac{90}{349}(n_{\text{B-L}})_{\text{total}}, \qquad n_\chi = \frac{58}{349}(n_{B-L})_{\text{total}} \quad (17)$$

Therefore,

$$\frac{n_\chi}{n_B} = \frac{58}{90}. \quad (18)$$

The expression for the relic of the asymmetric dark matter component is given by

$$\Omega_{\text{asy}} = n_\chi m_\chi / \rho_c, \quad (19)$$

where ρ_c is the critical density. For fully asymmetric dark matter $\Omega_{\text{DM}} = \Omega_{\text{asy}}$, so we have

$$\frac{\Omega_{\text{DM}}}{\Omega_B} = \frac{\Omega_{\text{asy}}}{\Omega_B} = \frac{n_\chi m_\chi}{m_B n_B} = \frac{58}{90} m_\chi. \quad (20)$$

From WMAP and Planck data, we have the ratio between dark matter density to baryonic matter density,

$$\frac{\Omega_{\text{DM}}}{\Omega_B} \sim 5. \quad (21)$$

Using Eqs. (20) and (21) we can get the dark matter mass for fully asymmetric dark matter to be $m_\chi = 7.76$ GeV. Now, if we consider that the dark matter is not fully asymmetric, instead it contains both symmetric and asymmetric components,

$$\Omega_{\text{DM}} h^2 = (\Omega_{\text{sym}} + \Omega_{\text{asy}}) h^2 = 0.12. \quad (22)$$

Therefore the percentage of the dark matter relic contributed by asymmetric part is given by

$$\text{ADM}(\%) = \frac{\Omega_{\text{asy}}}{\Omega_{\text{DM}}} \times 100 = \frac{\Omega_{\text{asy}}}{\Omega_{\text{sym}} + \Omega_{\text{asy}}} \times 100. \quad (23)$$

Using Eqs. (21) and (23) we have

$$\frac{\Omega_{\text{asy}}}{\Omega_B} = 5 \times \frac{\Omega_{\text{asy}}}{\Omega_{\text{sym}} + \Omega_{\text{asy}}} = 5 \times \frac{\text{ADM}(\%)}{100}. \quad (24)$$

Using Eqs. (20) and (23) we can write the dark matter mass for general scenario, where both symmetric and asymmetric component contributing to the dark matter relics as

$$m_\chi = \frac{90}{58} \times 5 \times \frac{\text{ADM}(\%)}{100}. \quad (25)$$

So depending on how much asymmetric relic contributes to the total DM relic, the mass of the dark matter will change accordingly from the above equation.

In this general scenario, the symmetric component contributing to the total relic is $(100 - \text{ADM})\%$. So we have

$$100 - \text{ADM}(\%) = \frac{\Omega_{\text{sym}} \times 100}{\Omega_{\text{sym}} + \Omega_{\text{asy}}} \\ = \frac{\Omega_{\text{sym}}}{\Omega_{\text{DM}}} \times 100 = \frac{\Omega_{\text{sym}} h^2}{0.12} \times 100, \\ \Rightarrow \Omega_{\text{sym}} h^2 = \frac{100 - \text{ADM}(\%)}{100} \times 0.12. \quad (26)$$

The relics of the symmetric component is determined by the thermal average of its annihilation cross section, given by

$$\Omega_{\text{sym}} h^2 = \frac{8.7661 \times 10^{-11}}{\sqrt{g_{*s}} J}, \quad (27)$$

where J is given by

$$J = \int_{x_f}^{\infty} \frac{\langle \sigma v \rangle_{\bar{\chi}\chi \to \phi\phi}}{x^2} dx. \quad (28)$$

where $\langle \sigma v \rangle_{\bar{\chi}\chi \to \phi\phi}$ is the thermally averaged cross section of the dominant annihilation process $\bar{\chi}\chi \to \phi\phi$ shown in the right panel of Fig. 3, which can be roughly estimated to be

$$\langle \sigma v \rangle_{\bar{\chi}\chi \to \phi\phi} \approx \frac{3}{4} \frac{\lambda_D^4}{16\pi m_\chi^2}. \quad (29)$$

The amount of annihilation can be very large or small depending on the value of λ_D. This fixes the contribution of the symmetric (and hence the asymmetric) component to the total DM relic density which in turn fixes the DM mass. Using Eqs. (26), (27), (28), and (29), we can determine the λ_D parameter with respect to ADM percentage (or equivalently DM mass), which is depicted by the dashed blue curve in the left panel of Fig. 6. Considering ADM

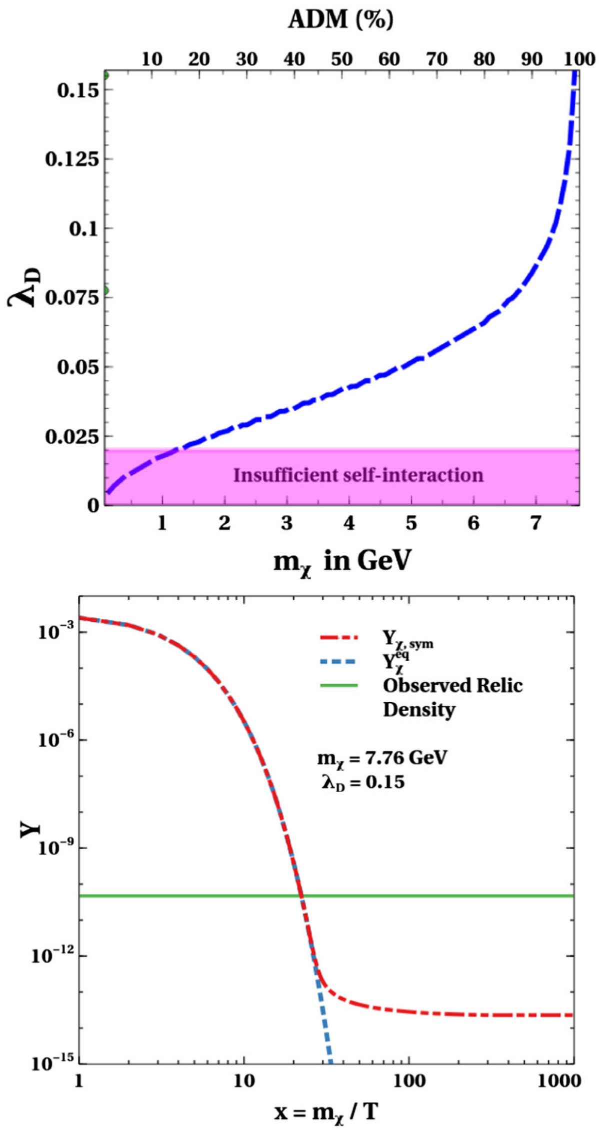

FIG. 6. Left: λ_D vs ADM(%) plot with corresponding DM mass in order to satisfy the correct relic density. The magenta shaded region is excluded due to insufficient DM self-interaction. Right: Underabundant relic of symmetric component of the DM as depicted by the dot-dashed red curve. The equilibrium number density is depicted by the dotted blue curve.

component to vary within 1–99.99%, the parameter λ_D varies within 0.005–0.15 and correspondingly allowed DM mass range is 0.07–7.76 GeV.

For fully asymmetric dark matter, i.e., ADM(%) > 99.99%, the relics of the symmetric component should be very small, which requires large λ_D ($\sim$0.15) for efficient annihilation of the symmetric component. Such a large λ_D in turn give rise to sufficient self-interaction among the DM particles mediated by the light scalar ϕ as depicted in the left panel of Fig. 3. We rule out the region $\lambda_D < 0.02$ (correspondingly $m_\chi < 1.3$ GeV) in the top panel of Fig. 6 due to insufficient self-interaction ($\sigma/m_{\rm DM} < 10^{-24}$ cm^2/GeV) which can not alleviate the small scale anomalies of ΛCDM. We elaborate the details of DM self-interaction in Sec. IV. For a fully ADM scenario, the evolution of the relic abundance of the symmetric component is shown in the right panel of Fig. 6 by solving the relevant Boltzmann equation for the comoving number density of the symmetric component $Y_{\chi,\rm sym} = \frac{n_{\chi,\rm sym}}{s}$, where $n_{\chi,\rm sym}$ is the actual number density and s is the entropy density. The Boltzmann equation is given by

$$\frac{dY_{\chi,\rm sym}}{dx} = -\frac{s(m_\chi)}{H(m_\chi)} \langle\sigma v\rangle_{\bar{\chi}\chi\to\phi\phi} (Y_{\chi,\rm sym}^2 - (Y_\chi^{eq})^2), \quad (30)$$

where $s(m_\chi)$ and $H(m_\chi)$ are the entropy density and the Hubble parameter as a function of DM mass defined as

$$s(m_\chi) = \frac{2\pi^2}{45} g_* m_\chi^3, \qquad H(m_\chi) = \frac{\pi}{\sqrt{90}} \frac{\sqrt{g_*}}{M_{pl}^r} m_\chi^2,$$

where $M_{pl}^r = 2.44 \times 10^{18}$ GeV is the reduced Planck mass and $Y_\chi^{\rm eq}$ is the equilibrium DM number density.

IV. DARK MATTER SELF-INTERACTION

The DM χ has elastic self-scattering, mediated by the light scalar ϕ as depicted by the Feynman diagram shown in left panel of Fig. 3, thanks to the interaction term $\lambda_D \bar{\chi}\chi\phi$ in the model Lagrangian given by Eq. (2). The scattering in nonrelativistic limit is well described by the attractive Yukawa potential,

$$V(r) = \frac{\lambda_D^2}{4\pi r} e^{-m_\phi r}. \quad (31)$$

To capture the relevant physics of forward scattering divergence, we define the transfer cross section σ_T as [31,37,45]

$$\sigma_T = \int d\Omega (1 - \cos\theta) \frac{d\sigma}{d\Omega}. \quad (32)$$

Depending on the masses of DM (m_χ) and the mediator (m_ϕ), as well as the relative velocity of the colliding particle (v) and the coupling (λ_D^2), we can identify three distinct regimes. The Born regime ($\lambda_D^2 m_\chi/(4\pi m_\phi) \ll 1, m_\chi v/m_\phi \geq 1$) is where the perturbative calculation holds good. Outside the Born regime, we have the classical regime ($\lambda_D^2 m_\chi/(4\pi m_\phi) \geq 1, m_\chi v/m_\phi \geq 1$) and the resonant regime ($\lambda_D^2 m_\chi/(4\pi m_\phi) \geq 1, m_\chi v/m_\phi \leq 1$) where nonperturbative and quantum-mechanical effects become important. The self-interaction cross sections in these regimes are listed in Appendix C. In the left panel of Fig. 7, we show the self-interaction allowed parameter space in $m_\chi - m_\phi$

plane obtained by constraining σ/m_χ in the correct ballpark from astrophysical data across different scales. We constrain σ/m_χ in the range 0.1–100 cm^2/g for dwarf galaxies ($v \sim 10$ km/s) as shown by the three shades of blue coloured region as indicated in the figure inset. The light magenta coloured region depicts the parameter space allowed for galaxies ($\sigma/m_\chi \sim 0.1$–$10\ \mathrm{cm}^2/\mathrm{g}$), while the green colored region depicts the parameter space allowed for clusters ($\sigma/m_\chi \sim 0.1$–$1\ \mathrm{cm}^2/\mathrm{g}$). The masses of DM and the mediator for which all three regions overlap will alleviate the small scale anomalies across all scales. The top (bottom) corner corresponds to the classical (Born) region, where the cross section depends on velocity trivially. The sandwiched region between these two is the so-called resonant region, where quantum mechanical resonances and antiresonances appear due to (quasi)bound state formation in the attractive potential. The resonances and antiresonances are most prominent at the dwarf scale due to the lower velocity of the DM particles and gradually becomes less prominent towards galaxy and cluster scales as DM velocity increases and less likely to be bounded. For a coupling λ_D, the condition $m_\chi v/m_\phi < 1$ dictates the onset of nonperturbative quantum mechanical effects, which is easily satisfied by smaller velocities. We have considered in the left panel of Fig. 7, $\lambda_D = 0.15$ which corresponds to fully asymmetric DM and also is just at the correct ballpark for sufficient self-interaction allowing maximum parameter space in the $m_\chi - m_\phi$ plane. For lower values of λ_D (which means DM is not fully asymmetric), the parameter space where desired cross sections can be obtained gradually decreases. For $\lambda_D < 0.02$, the obtained cross sections are below the ballpark of $\sigma/m_\chi \sim 0.1\ \mathrm{cm}^2/\mathrm{g}$, insufficient to alleviate the small-scale ΛCDM anomalies.

The self-scattering cross section per unit DM mass as a function of average collision velocity obtained from the model fits to data from dwarfs (red), low surface brightness (LSB) galaxies (blue), and clusters (green) [43,134] as shown in the bottom panel of Fig. 7. The purple curve corresponds to the benchmark point of fully asymmetric DM (m_χ = 7.76 GeV) with $m_\phi = 0.01$ GeV and $\lambda_D = 0.15$. We depict this point with a red star mark in Fig. 7 as well. The brown curve corresponds to the benchmark point of m_χ = 1.5 GeV with $m_\phi = 0.001$ GeV and $\lambda_D = 0.025$ which just cuts the mark to give sufficient self-interaction as shown in the top panel of Fig. 6. The magenta curve corresponds to an intermediate case with m_χ = 5 GeV, $m_\phi = 0.003$ GeV and $\lambda_D = 0.05$. Hence, it is clear from the bottom panel of Fig. 7 that the model can appreciably explain the astrophysical observation of velocity-dependent DM self-interaction.

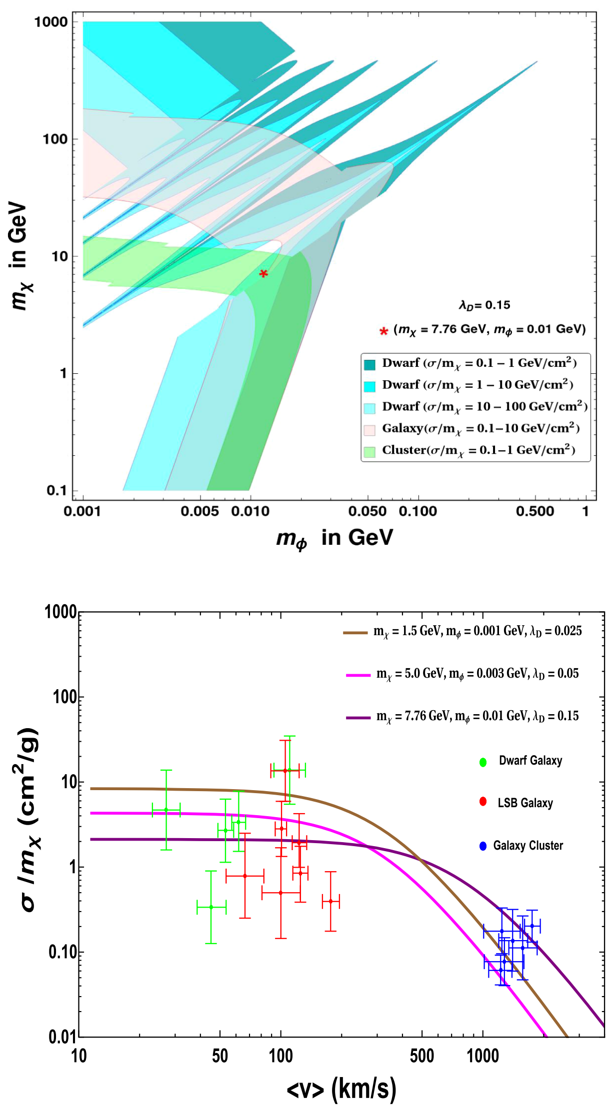

FIG. 7. Left: Self-interaction cross section in the range 0.1–1 cm^2/g for clusters ($v \sim 1000$ km/s), 0.1–10 cm^2/g for galaxies ($v \sim 200$ km/s.) and 0.1–1000 cm^2/g for dwarfs ($v \sim 10$ km/s). Right: The self-interaction cross section per unit mass of DM as a function of average collision velocity.

V. DM DIRECT SEARCH

The SIDM can be detected at terrestrial laboratories through $\phi - h$ mixing ($\theta_{\phi h}$), via its scattering off the target

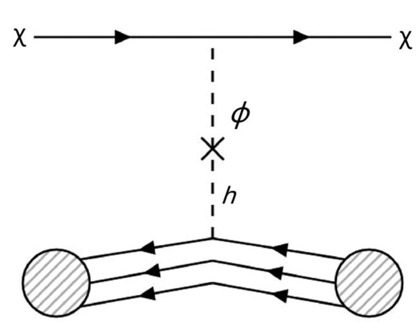

FIG. 8. Spin-independent DM-nucleon scattering via scalar mixing.

nuclei as depicted by the Feynman diagram shown in Fig. 8. the scattering cross section of DM per nucleon can be expressed as

$$\sigma_{SI}^{\phi-h} = \frac{\mu_r^2}{4\pi A^2}[Zf_p + (A-Z)f_n]^2, \tag{33}$$

where $\mu_r = \frac{m_\chi m_n}{m_\chi + m_n}$ is the reduced mass of the DM-nucleon system. Here m_n is the nucleon (proton or neutron) mass, A and Z are respectively the mass and atomic number of the target nucleus, f_p and f_n are the interaction strengths of proton and neutron with DM respectively, given as

$$f_{p,n} = \sum_{q=u,d,s} f_{T_q}^{p,n}\alpha_q \frac{m_{p,n}}{m_q} + \frac{2}{27} f_{TG}^{p,n} \sum_{q=c,t,b} \alpha_q \frac{m_{p,n}}{m_q}, \tag{34}$$

where

$$\alpha_q = \lambda_D \theta_{\phi h}\left(\frac{m_q}{v}\right)\left[\frac{1}{m_\phi^2} - \frac{1}{m_h^2}\right]. \tag{35}$$

In Eq. (34), the values of $f_{T_q}^{p,n}$ can be found in [135].

The mixing angle $\theta_{\phi h}$ can be derived in terms of the parameters $\lambda_{H\Phi}, \langle\Phi\rangle, v, m_\phi, m_h$. Depending on the value of $\lambda_{H\Phi}$, the $\phi - h$ mixing can be very small or large. $\theta_{\phi h}$ gets an upper bound from invisible Higgs decay (since typically $m_\phi < m_h$), while it has a conservative lower bound from the big bang nucleosynthesis (BBN)(since $\tau_\phi < \tau_{\rm BBN}$ in order to keep BBN predictions intact) [57]. Using Eqs. (34) and (35), the spin-independent DM-nucleon scattering cross section in Eq. (33), can be reexpressed as

$$\begin{aligned}\sigma_{\rm SI}^{\phi-h} = &\frac{{\mu_r}^2 \lambda_D \theta_{\phi h}^2}{\pi A^2}\left[\frac{1}{m_\phi^2} - \frac{1}{m_h^2}\right]^2 \\ &\times \left[Z\left(\frac{m_p}{v}\right)\left(f_{Tu}^p + f_{Td}^p + f_{Ts}^p + \frac{2}{9}f_{TG}^p\right)\right. \\ &\left.+ (A-Z)\left(\frac{m_n}{v}\right)\left(f_{Tu}^n + f_{Td}^n + f_{Ts}^n + \frac{2}{9}f_{TG}^n\right)\right]^2.\end{aligned} \tag{36}$$

Among the direct search experiments, CRESST-III [136] provides the most severe constraint on DM mass below 10 GeV, while XENON1T [137] provides the stringent constraints for DM mass above 10 GeV. In Fig. 9 these constraints are shown on the $m_\chi - m_\phi$ plane against the self-interaction favoured parameter space. The blue (purple) colored contours denote exclusion limits from XENON1T (CRESST-III) experiment for specific $\phi - h$ mixing parameter $\theta_{\phi h}$. The region to the left of each contour is excluded for that particular $\theta_{\phi h}$. It is seen from Fig. 9 that direct search experiments severely constrain the self-interaction favoured parameter space. In particular, for

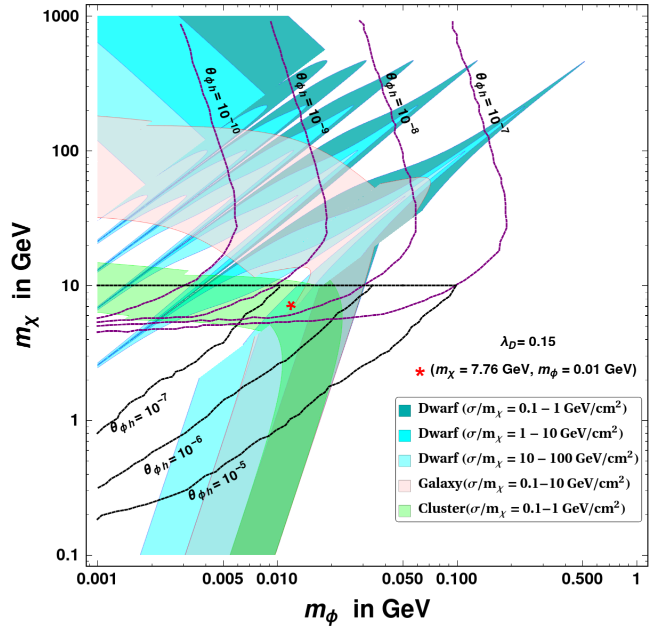

FIG. 9. Self-interaction allowed parameter space constrained by DM direct search in the plane of (m_χ) versus (m_ϕ).

$m_\chi = 7.76$ GeV and $m_\phi = 0.01$ GeV, $\theta_{\phi h} > 10^{-9}$ has already been ruled out. The red star mark depicts the benchmark point for fully asymmetric DM.

VI. NEUTRINO MASS

We explain neutrino mass through the higher-dimension operator,

$$\mathcal{L}_{\rm Dirac} = -y_1 \frac{\rho_1}{M_{X_1}^2}\bar{L}H\Phi'\nu_R - y_2 \frac{\rho_2}{M_{X_2}^2}\bar{L}H\Phi'\nu_R, \tag{37}$$

which is a Dirac-type dimension-five operator [90], where the trilinear coupling ρ has mass dimension. This operator shares the essential features of conventional Majorana-type dimension-five operator [13–16,138]. The Feynman graph for the operator is shown in Fig. 10. We get small Dirac neutrino mass after the SM-Higgs H and Φ' acquire VEV's $\langle H\rangle = v$ and $\langle\Phi'\rangle = w$, respectively,

$$M_\nu \simeq y_1 \frac{\rho_1 v w}{M_{X_1}^2} + y_2 \frac{\rho_2 v w}{M_{X_2}^2}. \tag{38}$$

Again, using the definition $f_{1,2} = \frac{\rho_{1,2}}{M_{X_{1,2}}}$, we can write

$$M_\nu \simeq y_1 f_1^2 v \frac{w}{\rho_1} + y_2 f_2^2 v \frac{w}{\rho_2}. \tag{39}$$

The mass of the heavy scalars $X_{1,2}$ i.e., $M_{X_{1,2}}$ is already decided from the requirement of Dirac leptogenesis to be of $\mathcal{O}(10^{10,11})$ GeV (see Sec. III). To explain the neutrino mass of the order of 0.1 eV, we pick a particular solution

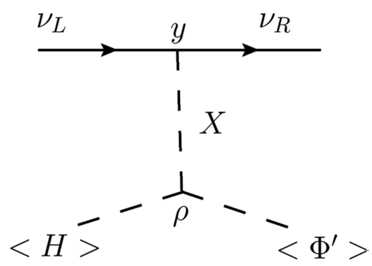

FIG. 10. Dirac neutrino mass generated through dimension-five operator.

for $y_{1,2}$ and $f_{1,2}$, say $y_1 = 2.2 \times 10^{-4}$, $y_2 = 1.1 \times 10^{-4}$ and $f_1 = 7.3 \times 10^{-5}$, $f_2 = 1.1$, which also explains successfully the lepton asymmetry in Sec. III. The other parameter which appear to achieve neutrino mass of $\mathcal{O}(10^{-10})$ GeV is $w = 10^{2.7}$ GeV.

Thus the parameters y, ρ and M_X are the bridging ligands for leptogenesis and neutrino mass. A typical set of parameters for which the model actually satisfies all the relevant phenomenology simultaneously can be given as $y_1 = 2.2 \times 10^{-4}$, $y_2 = 1.1 \times 10^{-4}$, $\rho_1 = 7.3 \times 10^5$ GeV, $\rho_2 = 1.1 \times 10^{11}$ GeV, $M_{\zeta_1} = 10^{10}$ GeV, $M_{\zeta_2} = 10^{11}$ GeV, $m_\phi = 0.003$–0.03 GeV, $\theta_{\phi h} \leq 10^{-9}$, $\omega = 10^{2.7}$ GeV, $v = 246$ GeV, $u \sim 10^{-2} - 10^{-3}$ GeV, $\lambda_H = 0.129$, $\lambda'_\phi \sim 1, \mu_1 \sim \mu_2 \sim -10^{-12}$ GeV, $\lambda_{H\Phi'} \sim 10^{-3}$, $\lambda_{H\Phi} \sim 10^{-10}$, $\lambda_{\Phi\Phi'} \sim 10^{-10}$. Note that in the above, we use a range of m_ϕ values (which give rise the correct order of DM self-interaction) for which we get a range of u values.

Corresponding to $\lambda = 1.5$ and $\lambda_{\eta H} = 1$ [see Eq. (4)] the mass scale of η is $M_\eta = 1.1 \times 10^4$ GeV.

The set of parameters which gives rise to the correct dark matter relic density is given as $m_\chi = 1.3$–7.76 GeV, $\lambda_D = 0.02 - 0.15$. Since we are considering the dominant asymmetric DM, the relic density is solely decided by these two parameters only.

VII. CONCLUSION

We extended the SM with two super heavy $SU(2)_L$ scalar doublets; X_i $(i = 1, 2)$, three right-handed neutrinos ν_{R_i} $(i = 1, 2, 3)$, two singlet scalars Φ, Φ', and a singlet Dirac fermion χ which represents the candidate of a self-interacting DM. We assumed a mass hierarchy among the heavy scalar doublets X_i, $i = 1, 2$. As a result the CP-violating out-of-equilibrium decay of the lightest heavy scalar generated a neutrino asymmetry in the visible sector. A part of the neutrino asymmetry is then transferred to the dark sector by a dimension-eight operator, $\mathcal{O}_8$, while a part of the remaining neutrino asymmetry gets converted to the baryon asymmetry by the electroweak sphaleron processes. This asymmetry transfer mechanism establishes a proportionality between the relic densities of dark matter and baryonic matter. The ratio between these two relic densities fixes the mass of the DM to be 7.76 GeV, if DM relic is fully asymmetric. However depending on the fractional contribution from symmetric and the asymmetric components, the DM mass can vary in the range 0.07–7.76 GeV. The light scalar mediator ϕ is introduced, not only facilitate velocity-dependent DM self-interaction to alleviate small-scale issues of ΛCDM, but also deplete the symmetric component of DM via the efficient annihilation process $\bar{\chi}\chi \to \phi\phi$. The requirement of sufficient self-interaction also rules out a region of available parameter space in terms of DM mass, further restricting it to 1.3–7.76 GeV. To realize sufficient DM self-interaction with this mass range of DM, the light scalar mass must be in the range 0.003–0.03 GeV. The self-interaction allowed parameter space has also been confronted with bounds from early Universe physics like BBN and present Universe physics like DM direct search and allowed parameter space from all phenomenological constraints has been specified. We have also explained the small Dirac neutrino mass at tree level through a dimension-five operator, where the mass of the heavy scalar X suppresses the weak scale. M_{X_1} is decided from the requirement of Dirac leptogenesis to be of $\mathcal{O}(10^{10})$ GeV (see Sec. III). To generate the desired lepton asymmetry, the branching ratio $B_L(X \to L\nu_R) \sim 0.9$, which requires that $f_1 = \frac{\rho_1}{M_{X_1}}$ and y_1 differ roughly by an order of magnitude. A typical solution $y_1 = 2.2 \times 10^{-4}$, $y_2 = 1.1 \times 10^{-4}$ and $f_1 = 7.3 \times 10^{-5}$, $f_2 = 1.1$ simultaneously satisfies both lepton asymmetry and neutrino mass. Therefore, the model at hand successfully explains the baryon asymmetry of the Universe along with neutrino mass and DM relic while providing a solution for small scale ΛCDM anomalies via DM self-interaction.

ACKNOWLEDGMENTS

M. D. acknowledges SERB CORE Grant No. CRG/2018/004971. N. S. acknowledges the support from Department of Atomic Energy (DAE)-Board of Research in Nuclear Sciences (BRNS), Government of India (Ref. No. 58/14/15/2021-BRNS/37220).

APPENDIX A: ASYMMETRY TRANSFER FROM VISIBLE TO DARK SECTOR

The asymmetry in the equilibrium number densities of particle n_i over antiparticle $\bar{n}_i$ can be written as

$$n_i - \bar{n}_i = \frac{g_i}{2\pi^2} \int_0^\infty dq\, q^2 \left[\frac{1}{e^{\frac{E_i(q)-\mu_i}{T}} \pm 1} - \frac{1}{e^{\frac{E_i(q)+\mu_i}{T}} \pm 1} \right], \quad \text{(A1)}$$

where the g_i is the internal degrees of freedom of the particle species i. In the above equation E_i and q_i represent the energy and momentum of the particle species i. In the approximation of a weakly interacting plasma, where $\beta\mu_i \ll 1$, $\beta \equiv 1/T$ (detailed discussions are given in [68,139]) we get,

$$n_i - \bar{n}_i \sim \frac{g_i T^3}{6} \times [2\beta\mu_i + \mathcal{O}((\beta\mu_i)^3)] \quad \text{for bosons}$$
$$\sim \frac{g_i T^3}{6} \times [\beta\mu_i + \mathcal{O}((\beta\mu_i)^3)] \quad \text{for fermions.} \tag{A2}$$

In this model, the asymmetry transfer operator is given by $\mathcal{O}_8 = \frac{1}{M_{\rm asy}^4}\bar{\chi}^2(LH)^2$ so the decoupling temperature of operator $\mathcal{O}_8$ is depends on the value of $M_{\rm asy}$. Since in this model the $B-L$ asymmetry is generated in the standard model sector which is required to be shared to the dark sector via $\mathcal{O}_8$ operator, we assume the decoupling temperature T_D to be $T_t > T_D > T_W$, where T_t is the temperature of thermal bath when the top quark decouples and T_W is the temperature when the W boson decouples from the thermal plasma. In this case the effective Lagrangian for Yukawa coupling is given by

$$\mathcal{L}_{Yukawa} = g^k_{e_i}\bar{e}_{iL}h^k e_{iR} + g^k_{u_i}\bar{u}_{iL}h^k u_{iR} + g^k_{d_i}\bar{d}_{iL}h^k d_{iR} + \text{H.c}, \tag{A3}$$

where $k = 1, 2, 3$ for three scalar mass eigenstates h_1, h_2 and h_3. Where h_1 is identified as standard model Higgs boson with mass 125 GeV. All these scalar fields are real so the above Lagrangian gives the following chemical equilibrium condition,

$$0 = \mu_{h^k} = \mu_{u_L} - \mu_{u_R} = \mu_{d_L} - \mu_{d_R} = \mu_{e_L} - \mu_{e_R}. \tag{A4}$$

After electroweak symmetry breaking the charged current interaction part of the SM Lagrangian is given by

$$\mathcal{L}^{(W)}_{\rm int} = gW^+_\mu \bar{u}_L\gamma^\mu d_L + gW^+_\mu e_L\gamma^\mu \bar{\nu}_{eL}. \tag{A5}$$

The charged current interactions remain in thermal equilibrium until the W boson decouples from thermal bath. Which gives the following chemical potential equations,

$$\mu_W = \mu_{u_L} - \mu_{d_L}, \tag{A6}$$

and

$$\mu_W = \mu_\nu - \mu_{e_L}. \tag{A7}$$

The electroweak sphalerons remain in thermal equilibrium until a temperature $T_{\rm sph} \gtrsim T_W$ leads to the following constraint,

$$\mu_{u_L} + 2\mu_{d_L} + \mu_\nu = 0. \tag{A8}$$

At a temperature below electroweak phase transition, the electric charge neutrality of the Universe holds. However, at the epoch $T_t > T_D > T_W$, the top quark is already decoupled from the thermal plasma and hence does not take part in the charge neutrality condition. Therefore, we get

$$Q = 4(\mu_{u_L} + \mu_{u_R}) + 6\mu_W - 3(\mu_{d_L} + \mu_{d_R} + \mu_{e_L} + \mu_{e_R}) = 0. \tag{A9}$$

Using Eq. (A2), the baryon number density n_B can be given as

$$n_B = \sum_i \mu_i \left(C_i Q^B_i \frac{g_i T^3\beta}{6} \right) \tag{A10}$$

where, i runs over two generations of up quarks and three generations of down quarks, C_i and Q^B_i count respectively the color and the baryon number of ith quark. Note that top quark is decoupled since it is heavy. Here, $g_i = 2$ is the internal degrees of freedom of each quark. Similarly, following Eq. (A2) the lepton number density n_L can be given as

$$n_L = \sum_i \mu_i \left(\frac{g_i T^3\beta}{6} \right), \tag{A11}$$

where, i runs over three generations of charged and neutral leptons. Now using the Eqs. (A4)–(A9), we can write the net baryon and lepton number density n_B and n_L as

$$n_B = -\frac{90}{29}\mu_\nu \tag{A12}$$

and

$$n_L = \frac{201}{29}\mu_\nu, \tag{A13}$$

where we have dropped the common factor $gT^3\beta/6$ as we are interested in ratio of densities, rather than their individual values. The net $B-L$ asymmetry in the visible sector is thus given by

$$(n_{B-L})_{\rm vis} = -\frac{291}{29}\mu_\nu. \tag{A14}$$

After sphaleron processes decouple at $T_{\rm sph}$, the baryon and lepton number densities would be conserved separately. As a result Eqs. (A4)–(A14) would remain valid at $T_{\rm sph} > M_W$. Once the sphaleron processes decouple, the ratio of n_B/n_{B-L} would be frozen. As a result from Eqs. (A12) and (A14), it can be written as

$$\frac{n_{B_{\rm final}}}{(n_{B-L})_{\rm vis}} = \frac{n_B}{(n_{B-L})_{\rm vis}} = \frac{30}{97} = 0.31 \tag{A15}$$

$$n_{B_{\rm final}} = 0.31(n_{B-L})_{\rm vis}. \tag{A16}$$

The operator $\mathcal{O}_8$ is in equilibrium until $T_D > T_{\rm sph}$ and equilibration of $\mathcal{O}_8$ gives the following constraint,

$$\mu_\chi = \mu_\nu. \tag{A17}$$

As a result the number density of dark matter χ (it is basically $B-L$ asymmetry in the dark sector) is given by, is given by

$$\begin{aligned} n_\chi &= 2\mu_\chi \frac{gT^3\beta}{6} \\ &= \frac{58}{291}(n_{B-L})_{\rm vis} \equiv (n_{B-L})_{\rm dark}. \end{aligned} \tag{A18}$$

APPENDIX B: DIAGONALIZATION OF THE SCALAR MASS MATRIX

For simplicity, let us denote the scalar mass matrix given in Eq. (9) as

$$\begin{pmatrix} A & B & C \\ B & D & E \\ C & E & F \end{pmatrix}. \tag{B1}$$

This mass matrix can be approximately block-diagonalized by the matrix

$$U = \begin{pmatrix} \cos\alpha & 0 & \sin\alpha \\ 0 & \cos\alpha & \sin\alpha \\ -\sin\alpha & -\sin\alpha & \cos\alpha \end{pmatrix} \tag{B2}$$

which is unitary up to order $\sin\alpha$. The block diagonalized matrix is of the form

$$\begin{pmatrix} A' & B' & 0 \\ B' & D' & 0 \\ 0 & 0 & F' \end{pmatrix}, \tag{B3}$$

where the elements of the above matrix are as follows:

$$\begin{aligned} A' &= A\cos^2\alpha + F - \sin^2\alpha - C\sin 2\alpha \\ B' &= B\cos^2\alpha + F\sin^2\alpha - \frac{1}{2}(C+E)\sin 2\alpha \\ D' &= D\cos^2\alpha + F\sin^2\alpha - E\sin 2\alpha \\ F' &= F\cos^2\alpha + (A+2B+D)\sin^2\alpha + (C+E)\sin 2\alpha. \end{aligned} \tag{B4}$$

The above diagonalization is obtained for the values of the angle α given by [ignoring $\mathcal{O}(\sin^2\alpha)$ terms]

$$\tan\alpha = \frac{C}{F-A-B} \quad (\text{or}) \frac{E}{F-B-D}. \tag{B5}$$

We assume the mass of ϕ to be extremely small compared to that of both ϕ' and h and it has very small mixing with both of them. We consider the induced VEV u of the field Φ to be very small compared to that of SM Higgs. In the limit of zero $\phi' - \phi$ as well as $h - \phi$ mixing, which is indeed guaranteed by the extremely tiny mixing parameter $\tan\alpha$ given by Eq. (B5), ϕ decouples from both ϕ' and h. The smallness of $\tan\alpha$ can be understood with the help of parameter values provided in Sec. VI *viz.* $\omega = 10^{2.7}$ GeV, $v = 246$ GeV, $u \sim 10^{-2}$ GeV, $\lambda'_\phi \sim 1, \lambda_H = 0.129$, $\mu_2 \sim -10^{-12}$, $\lambda'_\phi \sim 1$, $\lambda_{H\Phi'} \sim 10^{-3}$, $\lambda_{H\Phi} \sim 10^{-10}$, $m_\phi \sim 10^{-2}$ GeV, which gives $\tan\alpha \sim \mathcal{O}(10^{-12})$. The exact diagonalization is obtained by giving a consecutive (1,2) rotation to the squared mass matrix given in Eq. (B3) by the following Euler rotation matrix

$$O = \begin{pmatrix} \cos\beta & -\sin\beta & 0 \\ \sin\beta & \cos\beta & 0 \\ 0 & 0 & 1 \end{pmatrix}, \tag{B6}$$

where the $\phi' - h$ mixing is given by

$$\tan 2\beta = \frac{2B'}{D'-A'}. \tag{B7}$$

After complete diagonalization, we are left with an extremely light scalar $h_3 \approx \phi$ that mediates DM self-scattering and two other scalars with masses given by

$$\begin{aligned} m^2_{h_1} &= D'\cos^2\beta + A'\sin^2\beta + B\sin 2\beta \\ m^2_{h_2} &= A'\cos^2\beta + D'\sin^2\beta - B\sin 2\beta. \end{aligned} \tag{B8}$$

The mass eigenstate h_1 can be identified as the SM Higgs with mass $M_{h_1} = 125.18$ GeV, while h_2 as the second scalar that plays a role in generating the tiny neutrino mass.

APPENDIX C: DM SELF-INTERACTION CROSS SECTIONS AT LOW ENERGY

In the Born limit $[\lambda_D^2 m_\chi/(4\pi m_\phi) \ll 1]$,

$$\sigma_T^{\rm Born} = \frac{\lambda_D^4}{2\pi m_\chi^2 v^4}\left(ln\left(1+\frac{m_\chi^2 v^2}{m_\phi^2}\right) - \frac{m_\chi^2 v^2}{m_\phi^2 + m_\chi^2 v^2}\right) \tag{C1}$$

Outside the Born regime $(\lambda_D^2 m_\chi/(4\pi m_\phi) \geq 1)$, there are two distinct regions viz, the classical regime and the resonance regime. In the classical regime $(\lambda_D^2 m_\chi/(4\pi m_\phi \geq 1, m_\chi v/m_\phi \geq 1)$, the solutions for an attractive potential is given by [45,140,141]

$$\sigma_T^{\text{classical}} = \begin{cases} \frac{4\pi}{m_\phi^2}\beta^2 \ln(1+\beta^{-1}) & \beta \leq 10^{-1} \\ \frac{8\pi}{m_\phi^2}\beta^2/(1+1.5\beta^{1.65}) & 10^{-1} \leq \beta \leq 10^3 \\ \frac{\pi}{m_\phi^2}(\ln\beta + 1 - \frac{1}{2} ln^{-1}\beta) & \beta \geq 10^3, \end{cases} \tag{C2}$$

where $\beta = 2\lambda_D^2 m_\chi/(4\pi m_\phi)v^2$ In the resonant regime $(\lambda_D^2 m_\chi/(4\pi m_\phi) \geq 1, m_\chi v/m_\phi \leq 1)$, the quantum mechanical resonances and anti-resonance in σ_T appear due to (quasi-)bound states formation in the attractive potential. In the resonant regime, an analytical formula for σ_T is not available and one needs to solve the nonrelativistic Schrödinger equation by partial wave analysis. Instead, here we use the nonperturbative results obtained by approximating the Yukawa potential to be a Hulthen potential $(V(r) = \pm\frac{\lambda_D^2}{4\pi}\frac{\delta e^{-\delta r}}{1-e^{-\delta r}})$, which is given by [45]

$$\sigma_T^{\text{Hulthen}} = \frac{16\pi \sin^2\delta_0}{m_\chi^2 v^2}, \tag{C3}$$

where $l = 0$ phase shift δ_0 is given in terms of the Γ functions by

$$\delta_0 = \arg\left(i\Gamma\left(\frac{i m_\chi v}{k m_\phi}\right)/\Gamma(\lambda_+)\Gamma(\lambda_-)\right)$$
$$\lambda_\pm = 1 + \frac{i m_\chi v}{2k m_\phi} \pm \sqrt{\frac{\alpha_D m_\chi}{k m_\phi} - \frac{m_\chi^2 v^2}{4k^2 m_\phi^2}} \tag{C4}$$

and $k \approx 1.6$ is a dimensionless number.

[1] K. Abe *et al.*, Indication of Electron Neutrino Appearance from an Accelerator-produced Off-axis Muon Neutrino Beam, Phys. Rev. Lett. **107**, 041801 (2011).
[2] K. Abe *et al.*, Observation of Electron Neutrino Appearance in a Muon Neutrino Beam, Phys. Rev. Lett. **112**, 061802 (2014).
[3] Y. Abe *et al.* (Double Chooz Collaboration), Indication of Reactor $\bar{\nu}_e$ Disappearance in the Double Chooz Experiment, Phys. Rev. Lett. **108**, 131801 (2012).
[4] H. de Kerret *et al.* (Double Chooz Collaboration), First Double Chooz θ_{13} measurement via total neutron capture detection, Nat. Phys. **16**, 558 (2020).
[5] F. An *et al.* (Daya Bay Collaboration), Observation of Electron-Antineutrino Disappearance at Daya Bay, Phys. Rev. Lett. **108**, 171803 (2012).
[6] F. An *et al.* (Daya Bay Collaboration), Evolution of the Reactor Antineutrino Flux and Spectrum at Daya Bay, Phys. Rev. Lett. **118**, 251801 (2017).
[7] D. Adey *et al.* (Daya Bay Collaboration), Measurement of the Electron Antineutrino Oscillation with 1958 Days of Operation at Daya Bay, Phys. Rev. Lett. **121**, 241805 (2018).
[8] J. Ahn *et al.* (RENO Collaboration), Observation of Reactor Electron Antineutrino Disappearance in the RENO Experiment, Phys. Rev. Lett. **108**, 191802 (2012).
[9] P. Adamson *et al.* (MINOS Collaboration), Measurement of Neutrino and Antineutrino Oscillations Using Beam and Atmospheric Data in MINOS, Phys. Rev. Lett. **110**, 251801 (2013).
[10] P. Adamson *et al.* (MINOS Collaboration), Combined Analysis of ν_μ Disappearance and $\nu_\mu \to \nu_e$ Appearance in MINOS Using Accelerator and Atmospheric Neutrinos, Phys. Rev. Lett. **112**, 191801 (2014).
[11] I. Esteban, M.C. Gonzalez-Garcia, M. Maltoni, I. Martinez-Soler, and T. Schwetz, Updated fit to three neutrino mixing: Exploring the accelerator-reactor complementarity, J. High Energy Phys. 01 (2017) 087.
[12] S. Vagnozzi, E. Giusarma, O. Mena, K. Freese, M. Gerbino, S. Ho, and M. Lattanzi, Unveiling ν secrets with cosmological data: Neutrino masses and mass hierarchy, Phys. Rev. D **96**, 123503 (2017).
[13] P. Minkowski, $\mu \to e\gamma$ at a rate of one out of 10^9 muon decays?, Phys. Lett. B **67**, 421 (1977).
[14] T. Yanagida, Neutrino mass and horizontal symmetry, in *Proceedings of 1981 INS Symposium on Quark and Lepton Physics, Tokyo, Japan* (Institute for Nuclear Study, University of Tokyo, 1981), pp. 233–237.
[15] M. Gell-Mann, P. Ramond, and R. Slansky, Complex spinors and unified theories, Conf. Proc. C **790927**, 315 (1979), https://inspirehep.net/literature/9686.
[16] R. N. Mohapatra and G. Senjanovic, Neutrino Mass and Spontaneous Parity Nonconservation, Phys. Rev. Lett. **44**, 912 (1980).
[17] M. Magg and C. Wetterich, Neutrino mass problem and gauge hierarchy, Phys. Lett. **94B**, 61 (1980).
[18] G. Lazarides, Q. Shafi, and C. Wetterich, Proton lifetime and fermion masses in an SO(10) model, Nucl. Phys. **B181**, 287 (1981).
[19] R. N. Mohapatra and G. Senjanovic, Neutrino masses and mixings in gauge models with spontaneous parity violation, Phys. Rev. D **23**, 165 (1981).
[20] E. Ma and U. Sarkar, Neutrino Masses and Leptogenesis with Heavy Higgs Triplets, Phys. Rev. Lett. **80**, 5716 (1998).
[21] W. Konetschn and Kummer, Nonconservation of total lepton number with scalar bosons, Phys. Lett. **70B**, 433 (1977).
[22] J. Schechter and J. W. F. Valle, Neutrino masses in SU(2) $\otimes$ U(1) theories, Phys. Rev. D **22**, 2227 (1980).
[23] T. P. Cheng and L. F. Li, Neutrino masses, mixings, and oscillations in SU(2)×U(1) models of electroweak interactions, Phys. Rev. D **22**, 2860 (1980).

[24] R. Foot, H. Lew, X. G. He, and G. C. Joshi, Seesaw neutrino masses induced by a triplet of leptons, Z. Phys C **44**, 441 (1989).

[25] Y. Cai, J. H. García, M. A. Schmidt, A. Vicente, and R. R. Volkas, From the trees to the forest: A review of radiative neutrino mass models, Front. Phys. **5**, 63 (2017).

[26] G. Jungman, M. Kamionkowski, and K. Griest, Supersymmetric dark matter, Phys. Rep. **267**, 195 (1996).

[27] G. Bertone, D. Hooper, and J. Silk, Particle dark matter: Evidence, candidates and constraints, Phys. Rep. **405**, 279 (2005).

[28] G. Hinshaw *et al.* (WMAP Collaboration), Nine-Year Wilkinson Microwave Anisotropy Probe (WMAP) observations: Cosmological parameter results, Astrophys. J. Suppl. Ser. **208**, 19 (2013).

[29] Y. Akrami *et al.* (Planck Collaboration), Planck 2018 results. I. Overview and the cosmological legacy of Planck, Astron. Astrophys. **641**, A1 (2020).

[30] N. Aghanim *et al.* (Planck Collaboration), Planck 2018 results. VI. Cosmological parameters, Astron. Astrophys. **641**, A6 (2020).

[31] S. Tulin and H.-B. Yu, Dark matter self-interactions and small scale structure, Phys. Rep. **730**, 1 (2018).

[32] J. S. Bullock and M. Boylan-Kolchin, Small-scale challenges to the ΛCDM paradigm, Annu. Rev. Astron. Astrophys. **55**, 343 (2017).

[33] D. N. Spergel and P. J. Steinhardt, Observational Evidence for Self-Interacting Cold Dark Matter, Phys. Rev. Lett. **84**, 3760 (2000).

[34] E. D. Carlson, M. E. Machacek, and L. J. Hall, Self-interacting dark matter, Astrophys. J. **398**, 43 (1992).

[35] A. A. de Laix, R. J. Scherrer, and R. K. Schaefer, Constraints of self-interacting dark matter, Astrophys. J. **452**, 495 (1995).

[36] M. R. Buckley and P. J. Fox, Dark matter self-interactions and light force carriers, Phys. Rev. D **81**, 083522 (2010).

[37] J. L. Feng, M. Kaplinghat, and H.-B. Yu, Halo Shape and Relic Density Exclusions of Sommerfeld-Enhanced Dark Matter Explanations of Cosmic Ray Excesses, Phys. Rev. Lett. **104**, 151301 (2010).

[38] J. L. Feng, M. Kaplinghat, H. Tu, and H.-B. Yu, Hidden charged dark matter, J. Cosmol. Astropart. Phys. 07 (2009) 004.

[39] A. Loeb and N. Weiner, Cores in Dwarf Galaxies from Dark Matter with a Yukawa Potential, Phys. Rev. Lett. **106**, 171302 (2011).

[40] J. Zavala, M. Vogelsberger, and M. G. Walker, Constraining self-interacting dark matter with the Milky Way's dwarf spheroidals, Mon. Not. R. Astron. Soc. **431**, L20 (2013).

[41] M. Vogelsberger, J. Zavala, and A. Loeb, Subhaloes in self-interacting galactic dark matter haloes, Mon. Not. R. Astron. Soc. **423**, 3740 (2012).

[42] T. Bringmann, F. Kahlhoefer, K. Schmidt-Hoberg, and P. Walia, Strong Constraints on Self-Interacting Dark Matter with Light Mediators, Phys. Rev. Lett. **118**, 141802 (2017).

[43] M. Kaplinghat, S. Tulin, and H.-B. Yu, Dark Matter Halos as Particle Colliders: Unified Solution to Small-Scale Structure Puzzles from Dwarfs to Clusters, Phys. Rev. Lett. **116**, 041302 (2016).

[44] L. G. van den Aarssen, T. Bringmann, and C. Pfrommer, Is Dark Matter with Long-Range Interactions a Solution to All Small-Scale Problems of ΛCDM Cosmology?, Phys. Rev. Lett. **109**, 231301 (2012).

[45] S. Tulin, H.-B. Yu, and K. M. Zurek, Beyond collisionless dark matter: Particle physics dynamics for dark matter halo structure, Phys. Rev. D **87**, 115007 (2013).

[46] M. Kaplinghat, S. Tulin, and H.-B. Yu, Direct detection portals for self-interacting dark matter, Phys. Rev. D **89**, 035009 (2014).

[47] E. Del Nobile, M. Kaplinghat, and H.-B. Yu, Direct detection signatures of self-interacting dark matter with a light mediator, J. Cosmol. Astropart. Phys. 10 (2015) 055.

[48] C. Kouvaris, I. M. Shoemaker, and K. Tuominen, Self-interacting dark matter through the Higgs portal, Phys. Rev. D **91**, 043519 (2015).

[49] N. Bernal, X. Chu, C. Garcia-Cely, T. Hambye, and B. Zaldivar, Production regimes for self-interacting dark matter, J. Cosmol. Astropart. Phys. 03 (2016) 018.

[50] K. Kainulainen, K. Tuominen, and V. Vaskonen, Self-interacting dark matter and cosmology of a light scalar mediator, Phys. Rev. D **93**, 015016 (2016); **95**, 079901(E) (2017).

[51] T. Hambye and L. Vanderheyden, Minimal self-interacting dark matter models with light mediator, J. Cosmol. Astropart. Phys. 05 (2020) 001.

[52] M. Cirelli, P. Panci, K. Petraki, F. Sala, and M. Taoso, Dark matter's secret liaisons: Phenomenology of a dark U(1) sector with bound states, J. Cosmol. Astropart. Phys. 05 (2017) 036.

[53] F. Kahlhoefer, K. Schmidt-Hoberg, and S. Wild, Dark matter self-interactions from a general spin-0 mediator, J. Cosmol. Astropart. Phys. 08 (2017) 003.

[54] M. Dutta, S. Mahapatra, D. Borah, and N. Sahu, Self-interacting inelastic dark matter in the light of XENON1T excess, Phys. Rev. D **103**, 095018 (2021).

[55] D. Borah, M. Dutta, S. Mahapatra, and N. Sahu, Boosted self-interacting dark matter and XENON1T excess, Nucl. Phys. **B979**, 115787 (2022).

[56] D. Borah, M. Dutta, S. Mahapatra, and N. Sahu, Self-interacting dark matter via right handed neutrino portal, Phys. Rev. D **105**, 015004 (2022).

[57] D. Borah, M. Dutta, S. Mahapatra, and N. Sahu, Singlet-doublet self-interacting dark matter and neutrino mass, Phys. Rev. D **105**, 075019 (2022).

[58] D. Borah, M. Dutta, S. Mahapatra, and N. Sahu, Unified origin of dark matter self-interactions and low scale leptogenesis, arXiv:2112.14786.

[59] O. Azzolini *et al.* (CUPID-0 Collaboration), First Result on the Neutrinoless Double- β Decay of ^{82}Se with CUPID-0, Phys. Rev. Lett. **120**, 232502 (2018).

[60] K. Dick, M. Lindner, M. Ratz, and D. Wright, Leptogenesis with Dirac Neutrinos, Phys. Rev. Lett. **84**, 4039 (2000).

[61] H. Murayama and A. Pierce, Realistic Dirac Leptogenesis, Phys. Rev. Lett. **89**, 271601 (2002).

[62] M. Boz and N. K. Pak, Dirac leptogenesis and anomalous U(1), Eur. Phys. J, C **37**, 507 (2004).

[63] S. Abel and V. Page, Affleck-Dine (pseudo)-Dirac neutrinogenesis, J. High Energy Phys. 05 (2006) 024.
[64] D. G. Cerdeno, A. Dedes, and T. E. J. Underwood, The minimal phantom sector of the standard model: Higgs phenomenology and Dirac leptogenesis, J. High Energy Phys. 09 (2006) 067.
[65] B. Thomas and M. Toharia, Phenomenology of Dirac neutrinogenesis in split supersymmetry, Phys. Rev. D **73**, 063512 (2006).
[66] B. Thomas and M. Toharia, Lepton flavor violation and supersymmetric Dirac leptogenesis, Phys. Rev. D **75**, 013013 (2007).
[67] D. E. Kaplan, M. A. Luty, and K. M. Zurek, Asymmetric dark matter, Phys. Rev. D **79**, 115016 (2009).
[68] W.-Z. Feng, P. Nath, and G. Peim, Cosmic coincidence and asymmetric dark matter in a Stueckelberg extension, Phys. Rev. D **85**, 115016 (2012).
[69] M. Ibe, S. Matsumoto, and T. T. Yanagida, The GeV-scale dark matter with B–L asymmetry, Phys. Lett. B **708**, 112 (2012).
[70] W.-Z. Feng, A. Mazumdar, and P. Nath, Baryogenesis from dark matter, Phys. Rev. D **88**, 036014 (2013).
[71] N. Narendra, S. Patra, N. Sahu, and S. Shil, Baryogenesis via leptogenesis from asymmetric dark matter and radiatively generated neutrino mass, Phys. Rev. D **98**, 095016 (2018).
[72] A. D. Sakharov, Violation of *CP* invariance, C asymmetry, and baryon asymmetry of the universe, Pis'ma Zh. Eksp. Teor. Fiz. **5**, 32 (1967), https://inspirehep.net/literature/51345; Usp. Fiz. Nauk **161**, 61 (1991).
[73] A. D. Sakharov, Violation of CP Invariance, C asymmetry, and baryon asymmetry of the universe, JETP Lett. **5**, 24 (1967), https://inspirehep.net/literature/51345.
[74] M. Fukugita and T. Yanagida, Barygenesis without grand unification, Phys. Lett. B **174**, 45 (1986).
[75] M. A. Luty, Baryogenesis via leptogenesis, Phys. Rev. D **45**, 455 (1992).
[76] R. N. Mohapatra and X. Zhang, Electroweak baryogenesis in left-right-symmetric models, Phys. Rev. D **46**, 5331 (1992).
[77] A. Acker, H. Kikuchi, E. Ma, and U. Sarkar, CP violation and leptogenesis, Phys. Rev. D **48**, 5006 (1993).
[78] M. Flanz, E. A. Paschos, and U. Sarkar, Baryogenesis from a lepton asymmetric universe, Phys. Lett. B **345**, 248 (1995).
[79] M. Flanz, E. A. Paschos, U. Sarkar, and J. Weiss, Baryogenesis through mixing of heavy Majorana neutrinos, Phys. Lett. B **389**, 693 (1996); M. Plumacher, Baryogenesis and lepton number violation, Z. Phys. C **74**, 549 (1997).
[80] W. Buchmuller, P. Di Bari, and M. Plumacher, Leptogenesis for pedestrians, Ann. Phys. (Amsterdam) **315**, 305 (2005).
[81] J. Faridani, S. Lola, P. J. O'Donnell, and U. Sarkar, Scale of leptogenesis, Eur. Phys. J. C **7**, 543 (1999); R. Barbieri, P. Creminelli, A. Strumia, and N. Tetradis, Baryogenesis through leptogenesis, Nucl. Phys. **B575**, 61 (2000).
[82] G. F. Giudice, A. Notari, M. Raidal, A. Riotto, and A. Strumia, Towards a complete theory of thermal leptogenesis in the SM and MSSM, Nucl. Phys. **B685**, 89 (2004).
[83] N. Sahu and U. Sarkar, Leptogenesis bound on neutrino masses in left-right symmetric models with spontaneous D-parity violation, Phys. Rev. D **74**, 093002 (2006).
[84] A. Abada, S. Davidson, A. Ibarra, F. X. Josse-Michaux, M. Losada, and A. Riotto, Flavour matters in leptogenesis, J. High Energy Phys. 09 (2006) 010.
[85] A. Pilaftsis and T. E. J. Underwood, Resonant leptogenesis, Nucl. Phys. **B692**, 303 (2004).
[86] A. Pilaftsis and T. E. J. Underwood, Electroweak-scale resonant leptogenesis, Phys. Rev. D **72**, 113001 (2005).
[87] W. Buchmuller and M. Plumacher, Neutrino masses and the baryon asymmetry, Int. J. Mod. Phys. A **15**, 5047 (2000).
[88] K. Dick, M. Lindner, M. Ratz, and D. Wright, Leptogenesis with Dirac Neutrinos, Phys. Rev. Lett. **84**, 4039 (2000).
[89] D. G. Cerdeno, A. Dedes, and T. E. J. Underwood, The Minimal Phantom Sector of the Standard Model: Higgs Phenomenology and Dirac leptogenesis, J. High Energy Phys. 09 (2006) 067.
[90] P. H. Gu and H. J. He, Neutrino mass and baryon asymmetry from Dirac seesaw, J. Cosmol. Astropart. Phys. 12 (2006) 010.
[91] P. H. Gu, H. J. He, and U. Sarkar, Realistic neutrinogenesis with radiative vertex correction, Phys. Lett. B **659**, 634 (2008).
[92] H. Murayama and A. Pierce, Realistic Dirac Leptogenesis, Phys. Rev. Lett. **89**, 271601 (2002).
[93] B. Thomas and M. Toharia, Phenomenology of Dirac neutrinogenesis in split supersymmetry, Phys. Rev. D **73**, 063512 (2006).
[94] D. Borah and A. Dasgupta, Common origin of neutrino mass, dark matter and Dirac leptogenesis, J. Cosmol. Astropart. Phys. 12 (2016) 034.
[95] P. F. Perez, C. Murgui, and A. D. Plascencia, Common origin of neutrino mass, dark matter and Dirac leptogenesis, Phys. Rev. D **104**, 055007 (2021).
[96] S. Nussinov, Technocosmology: Could a technibaryon excess provide A 'natural' missing mass candidate?, Phys. Lett. **165B**, 55 (1985).
[97] K. Griest and D. Seckel, Cosmic asymmetry, neutrinos and the Sun, Nucl. Phys. **B283**, 681 (1987); **B296**, 1034 (1988).
[98] R. S. Chivukula and T. P. Walker, Technicolor cosmology, Nucl. Phys. **B329**, 445 (1990).
[99] S. Dodelson, B. R. Greene, and L. M. Widrow, Baryogenesis, dark matter and the width of the Z, Nucl. Phys. **B372**, 467 (1992).
[100] S. M. Barr, Baryogenesis, sphalerons and the cogeneration of dark matter, Phys. Rev. D **44**, 3062 (1991).
[101] D. B. Kaplan, A Single Explanation for Both the Baryon and Dark Matter Densities, Phys. Rev. Lett. **68**, 741 (1992).
[102] T. Inui, T. Ichihara, Y. Mimura, and N. Sakai, Cosmological baryon asymmetry in supersymmetric standard models and heavy particle effects, Phys. Lett. B **325**, 392 (1994).
[103] S. D. Thomas, Baryons and dark matter from the late decay of a supersymmetric condensate, Phys. Lett. B **356**, 256 (1995).
[104] R. Kitano and I. Low, Dark matter from baryon asymmetry, Phys. Rev. D **71**, 023510 (2005).

[105] K. Agashe and G. Servant, Baryon number in warped GUTs: Model building and (dark matter related) phenomenology, J. Cosmol. Astropart. Phys. 02 (2005) 002.
[106] N. Cosme, L. Lopez Honorez, and M. H. G. Tytgat, Leptogenesis and dark matter related?, Phys. Rev. D **72**, 043505 (2005).
[107] G. R. Farrar and G. Zaharijas, Dark Matter and the Baryon Asymmetry, Phys. Rev. Lett. **96**, 041302 (2006).
[108] R. Kitano, H. Murayama, and M. Ratz, Unified origin of baryons and dark matter, Phys. Lett. B **669**, 145 (2008).
[109] E. Nardi, F. Sannino, and A. Strumia, Decaying dark matter can explain the $e^{\pm}$ excesses, J. Cosmol. Astropart. Phys. 01 (2009) 043.
[110] H. An, S. L. Chen, R. N. Mohapatra, and Y. Zhang, Leptogenesis as a common origin for matter and dark matter, J. High Energy Phys. 03 (2010) 124.
[111] T. Cohen and K. M. Zurek, Leptophilic Dark Matter from the Lepton Asymmetry, Phys. Rev. Lett. **104**, 101301 (2010).
[112] J. Shelton and K. M. Zurek, Darkogenesis: A baryon asymmetry from the dark matter sector, Phys. Rev. D **82**, 123512 (2010).
[113] H. Davoudiasl, D. E. Morrissey, K. Sigurdson, and S. Tulin, Hylogenesis: A Unified Origin for Baryonic Visible Matter and Antibaryonic Dark Matter, Phys. Rev. Lett. **105**, 211304 (2010).
[114] K. Kohri, A. Mazumdar, and N. Sahu, Inflation, baryogenesis and gravitino dark matter at ultra low reheat temperatures, Phys. Rev. D **80**, 103504 (2009).
[115] K. Kohri, A. Mazumdar, N. Sahu, and P. Stephens, Probing unified origin of dark matter and baryon asymmetry at PAMELA/Fermi, Phys. Rev. D **80**, 061302 (2009).
[116] K. Kohri and N. Sahu, Constraining the cogenesis of visible and dark matter with AMS-02 and Xenon-100, Phys. Rev. D **88**, 103001 (2013).
[117] M. Ibe, S. Matsumoto, and T. T. Yanagida, The GeV-scale dark matter with B–L asymmetry, Phys. Lett. B **708**, 112 (2012).
[118] M. L. Graesser, I. M. Shoemaker, and L. Vecchi, Asymmetric WIMP dark matter, J. High Energy Phys. 10 (2011) 110.
[119] D. Hooper, J. March-Russell, and S. M. West, Asymmetric sneutrino dark matter and the $\Omega(b)/\Omega(DM)$ puzzle, Phys. Lett. B **605**, 228 (2005).
[120] H. Iminniyaz, M. Drees, and X. Chen, Relic abundance of asymmetric dark matter, J. Cosmol. Astropart. Phys. 07 (2011) 003.
[121] N. Haba, S. Matsumoto, and R. Sato, Sneutrino inflation with asymmetric dark matter, Phys. Rev. D **84**, 055016 (2011).
[122] Z. Kang, J. Li, T. Li, T. Liu, and J. M. Yang, The maximal $U(1)_L$ inverse seesaw from $d = 5$ operator and oscillating asymmetric Sneutrino dark matter, Eur. Phys. J. C **76**, 270 (2016).
[123] C. Arina and N. Sahu, Asymmetric inelastic inert doublet dark matter from triplet scalar leptogenesis, Nucl. Phys. **B854**, 666 (2012).
[124] C. Arina, J. O. Gong, and N. Sahu, Unifying darko-leptogenesis with scalar triplet inflation, Nucl. Phys. **B865**, 430 (2012).
[125] C. Arina, R. N. Mohapatra, and N. Sahu, Co-genesis of matter and dark matter with vector-like fourth generation leptons, Phys. Lett. B **720**, 130 (2013).
[126] K. Petraki and R. R. Volkas, Review of asymmetric dark matter, Int. J. Mod. Phys. A **28**, 1330028 (2013).
[127] K. M. Zurek, Asymmetric dark matter: Theories, signatures, and constraints, Phys. Rep. **537**, 91 (2014).
[128] E. Ma and U. Sarkar, Neutrino Masses and Leptogenesis with Heavy Higgs Triplets, Phys. Rev. Lett. **80**, 5716 (1998).
[129] N. Narendra, N. Sahoo, and N. Sahu, Dark matter assisted Dirac leptogenesis and neutrino mass, Nucl. Phys. **B936**, 76 (2018).
[130] W. Buchmuller and M. Plumacher, Matter–antimatter asymmetry and neutrino properties, Phys. Rep. **320**, 329 (1999).
[131] W. Buchmuller, P. Di Bari, and M. Plumacher, Leptogenesis for pedestrians, Ann. Phys. (Amsterdam) **315**, 305 (2005).
[132] G. F. Giudice, A. Notari, M. Raidal, A. Riotto, and A. Strumia, Towards a complete theory of thermal leptogenesis in the SM and MSSM, Nucl. Phys. **B685**, 89 (2004).
[133] N. Narendra, N. Sahu, and S. Shil, Dark matter to baryon ratio from scalar triplets decay in type-II seesaw, Eur. Phys. J. C **81**, 1098 (2021).
[134] A. Kamada, H. J. Kim, and T. Kuwahara, Maximally self-interacting dark matter: Models and predictions, J. High Energy Phys. 12 (2020) 202.
[135] J. R. Ellis, A. Ferstl, and K. A. Olive, Reevaluation of the elastic scattering of supersymmetric dark matter, Phys. Lett. B **481**, 304 (2000).
[136] A. Abdelhameed *et al.* (CRESST Collaboration), First results from the CRESST-III low-mass dark matter program, Phys. Rev. D **100**, 102002 (2019).
[137] E. Aprile *et al.* (XENON Collaboration), Dark Matter Search Results from a One Ton-Year Exposure of XENON1T, Phys. Rev. Lett. **121**, 111302 (2018).
[138] S. Weinberg, Baryon and Lepton Nonconserving Processes, Phys. Rev. Lett. **43**, 1566 (1979).
[139] E. W. Kolb and M. S. Turner, *The Early Universe* (CRC Press, Boca Raton, FL, 1990), Vol. 69, 10.1201/9780429492860.
[140] S. Tulin, H.-B. Yu, and K. M. Zurek, Resonant Dark Forces and Small Scale Structure, Phys. Rev. Lett. **110**, 111301 (2013).
[141] S. A. Khrapak, A. V. Ivlev, G. E. Morfill, and S. K. Zhdanov, Scattering in the Attractive Yukawa Potential in the Limit of Strong Interaction, Phys. Rev. Lett. **90**, 225002 (2003).